Patterning total mercury distribution in coastal podzolic soils from an Atlantic area: Influence of pedogenetic processes and soil components

A. Gómez-Armesto [a,b,*], M. Méndez-López [a,b], P. Marques [c], X. Pontevedra-Pombal [d], F. Monteiro [c,†], M. Madeira [c], M. Arias-Estévez [a,b], J.C. Nóvoa-Muñoz [a,b]

[a] Universidade de Vigo, Departamento de Bioloxía Vexetal e Ciencia do Solo, Área de Edafoloxía e Química Agrícola, Facultade de Ciencias. As Lagoas s/n, 32004 Ourense, Spain
[b] Campus da Auga, Universidade de Vigo, Laboratorio de Tecnoloxía e Diagnose Ambiental. Rúa Canella da Costa Vella 12, 32004 Ourense, Spain
[c] CEF - Centro de Estudos Florestais, Instituto Superior de Agronomia, Universidade de Lisboa, Tapada da Ajuda, 1349-017 Lisboa, Portugal
[d] Departamento de Edafoloxía e Química Agrícola, Facultade de Bioloxía, Universidade de Santiago de Compostela. Rúa Lope Gómez de Marzoa s/n, 15786 Santiago de Compostela, Spain

A B S T R A C T

Soils are the main Hg reservoir in the terrestrial ecosystems where it is deposited via wet or dry deposition and litterfall. Once on the soil surface, different biogeochemical routes will determine the fate of Hg and the role of terrestrial ecosystems as a Hg source or sink. The specific chemical and physical characteristics of Podzols and podzolic soils contribute to the accumulation of Hg in their illuvial horizons, avoiding its leaching to groundwater. The geographical location, state of pedogenesis, soil age, abundance of carrier phases and physical properties can affect the presence and distribution of Hg in soils. Therefore, understand and relate these factors with the behavior of Hg in Podzols and podzolic soils is key to define the role of this type of soil in the terrestrial Hg cycle. In this work, ten podzolic soil profiles were collected in an Atlantic coastal forest area of Portugal and analyzed for the main physico-chemical properties and Hg content to assess the influence of the intensity of podzolization in the Hg depth distribution. Three different patterns of Hg distribution in the studied Podzols, depending on the predominance of atmospheric deposition or the intensity of podzolization, have been defined. The pattern I showed the maximum Hg contents in the surface A horizons (12.9–23.5 μg kg^{-1}), pattern II exhibited the highest peaks in the subsurface illuvial horizons (2.3–17.3 μg kg^{-1}) and pattern III presented an even distribution of Hg through the soil profile. We found that dissolved organic matter (DOM) is the main carrier of Hg in the A and E horizons, whereas metal(Al, Fe)-humus complexes and/or oxyhydroxides contribute to immobilizing Hg in the illuvial horizons (Bh, Bs and Bhs). The principal component regression (PCR) analysis predicted satisfactorily the Hg distribution through soil organic matter and Al and Fe oxyhydroxides. The Hg immobilized in the subsurface layers of Podzols is retained in the long term, avoiding its migration to other components of terrestrial ecosystems where it could cause serious environmental damage such as groundwater and superficial waters.

1. Introduction

The knowledge of the presence, distribution and fate of mercury (Hg) in soils is key to understand the role of terrestrial ecosystems in the global biogeochemical Hg cycle. Depending on the balance between inputs and emissions from soils, they can act indistinctively as a source or sink (Jiskra et al., 2015; Obrist et al., 2014; Peretyazhko et al., 2006; Poissant and Casimir, 1998), a fact that will determine their function on

the Hg exchanges among biosphere components worldwide. Because of the wide variety and distribution of soils globally, the deposition sources can geographically differ between locations mostly due to climatic conditions and vegetation (Wang et al., 2019).

Mercury can reach soils through different mechanisms both from natural and anthropogenic sources, including senescence of vegetation at different deposition rates (Guédron et al., 2013; Jiskra et al., 2015; Sheehan et al., 2006), direct wet or dry deposition (Enrico et al., 2016;

---

* Corresponding author.
  E-mail address: angomez@uvigo.es (A. Gómez-Armesto).
† Deceased.

Rutter et al., 2011) and even weathering of the soil parent material. However, in areas far from emission sources and not naturally Hg enriched, the predominant origin of Hg is the atmosphere, which causes its preferential accumulation in the uppermost soil horizons (up to 30–50 cm), mainly bound to the sulfur groups of the organic matter (Skyllberg et al., 2006; Khwaja et al., 2006). Because of the primarily atmospheric provenance, soils are considered to accomplish the role of Hg sink in terrestrial environments, accounting for 250–1000 Gg of the organically bound Hg (Horowitz et al., 2014).

Mercury deposited over the surface of soils can be exposed to different biogeochemical routes that will determine either its transference to other environmental compartments or its retention in the soil. Particularly, the Hg depth distribution in different soil profiles and pedosequences can be determined by a variety of factors such as the abundance and affinity for carrier phases, the physical characteristics, and the age or stage of pedogenesis.

Firstly, the presence of certain soil components can either increase the Hg migration through the soil profile or reduce it causing some Hg immobilization in certain soil layers. The most common soil components involved in Hg biogeochemistry are organic matter complexes (Khwaja et al., 2006; Qian et al., 2002; Schlüter, 1997; Schuster, 1991), Al and Fe compounds such as metal(Al, Fe)-humus complexes or Al and Fe oxyhydroxides (Guédron et al., 2018; Jiskra et al., 2012; Roulet and Lucotte, 1995; Sarkar et al., 1999) and clay minerals (Hamilton et al., 1995; Sarkar et al., 2000).

Secondly, the mobility of Hg through the soil profile could be influenced by soil physical and hydraulic properties such as the texture. The migration of Hg and other soil components is strongly enhanced in coarse-textured soils, characterized by high sand contents and low amounts of silt and clay-sized particles (Biester et al., 2002; Sauer et al., 2008; Grand and Lavkulich, 2011; Rothstein et al., 2018), allowing Hg and other contaminants to reach other environmental compartments like groundwater or superficial waters. On the contrary, clay-sized particles not only slow down the migration of water through the soil profile but also act retaining Hg because of their higher reactivity due to the greater specific surface area, negative charge (Qin et al., 2014; Yin et al., 2016) as well as moderate content of organic matter (Gómez-Armesto et al. 2020a). However, clay-sized particles show little influence on the hydraulic conductivity when aggregated, allowing water circulation through the macroporous space, as for ferralitic soils (Do Valle et al., 2005; Fiorentino et al., 2011). This is not the case of the illuvial horizons, where the pore obstruction by clay particles and organic matter reduces the soil permeability at the bottom of these soil profiles (Fritsch et al., 2011; Gómez-Armesto et al., 2018; Gómez-Armesto et al., 2020a).

In the specific case of Podzols, Hg can be leached downwards the soil profile from the surface horizons together with other soil compounds, such as dissolved organic matter (DOM), Al and Fe colloidal compounds (Guédron et al., 2009; Navrátil et al., 2014; Richardson et al., 2018). Podzols are characterized by an ash-grey eluvial horizon (E) underlying by a reddish-brown to dark illuvial horizon (Bh, Bs or Bhs). The eluvial horizons are impoverished in soil organic matter, Al and Fe compounds, while illuvial horizons are enriched in them (Sauer et al., 2007). Podzols usually develop over coarse-textured parent materials poor in base cations and rich in quartz (Lundström et al., 2000). Therefore, both the presence and abundance of Hg carrier phases and the texture of this type of soil regulate the migration of Hg and other soil compounds through the soil profile.

In highly permeable surface sandy horizons of Podzols, the migration of Hg to deeper soil layers is enhanced and thus, a gradual decrease of Hg concentrations with increasing depth is expected (Biester et al., 2002). However, below the eluvial horizons, the downwards transport of Hg in the soil solution would be reduced due to the presence and accumulation of soil components, such as organic matter, Al and Fe compounds, able to retain Hg in the long term, avoiding its transport to other environmental systems and thus reducing its toxicity. Therefore,

the specific objectives of the present study were to (1) determine the Hg concentration and its vertical distribution in ten podzolic soil profiles characterized by an extremely high content of sand in an Atlantic coastal area of Portugal, (2) relate it to the main soil processes and components that characterize podzolization, and (3) search for the main soil compounds implied in the Hg patterns observed in these soils.

2. Material and methods

2.1. Study area

The soils under investigation are located in the Leiria National Forest (39°42′41.66′′-39°52′19.90′′N; 9°02′19.83′′-8°53′43.56′′W; Marinha Grande, Portugal), a national pine forest managed since 1879. The climate of the area is of Mediterranean type, tempered by an oceanic influence; the mean annual air humidity is about 84%. Mean annual precipitation ranges 710–910 mm, and the mean annual air temperature is 14.1 °C, ranging from a mean of 9.5 °C in December to 19.4 °C in August (INMG, 1991). The landscape is flat to undulating and the altitude ranges 10–130 m. Soils of the National Forest, Arenossols, Podzols and intergrades (Monteiro et al., 2015), are developed over quaternary sedimentary rocks (quartz sands), which in small areas overly Pliocene formations (Zbyszewski and Torre de Assunção, 1965). Current forest vegetation includes a maritime pine (*Pinus pinaster* Ait.) plantation with a density of 170–180 trees ha^{-1}, associated with shrubs, namely *Calluna vulgaris* (L.) Hull, *Cistus salviifolius* L., *Halimium calycinum* (L.) K. Koch, *Ulex europaeus* subsp. *latebracteatus* L., *Phillyrea angustifoli*a L. and *Pteridium aquilinum* (L) Kuhn.

2.2. Soil sampling

Following a previous study to assess the characterization, classification and distribution of Podzols in the Leiria National Forest (Monteiro et al., 2015), ten soil profiles with podzolic features were chosen for the present study. Eight pedons (P.1, P.2, P.3, P.6, P.8, P.20, P.21, P.25) are developed on sand dunes, whereas two (P.10, P.26) are developed on dunes overlying Pliocene formations. All the soil sampling sites are located in a flat relief with slopes ranging from flat to very gentle slope (<2%) according to FAO (2006). At any sampling site, a pit was excavated and samples from each horizon identified were taken with a plastic garden trowel, which was rinsed twice with a diluted HNO$_3$ solution and then dried between sample collection. In total, a population of 67 samples was collected. Soil samples were stored in plastic bags and transported to the laboratory in a portable fridge at 4 °C. Once in the laboratory, after plant debris, stones and other large particles removal, samples were disaggregated, air-dried at room temperature, and sieved using a 2-mm mesh.

2.3. Physico-chemical and mineralogical characterization of soil samples

General characterization of bulk soil samples (<2 mm) of the different horizons included the particle-size distribution applying the internationally-recognized pipette method (Gee and Bauder, 1986) with previous oxidation of soil organic matter by using 30% H$_2$O$_2$. In addition, soil pH in water (pH$_w$) and 0.1 M KCl solution (pH$_K$) using a 1:2.5 soil:solution ratio, and total C and N contents were determined in finely milled samples by using an autoanalyzer (Fisons EA 1108, Mt Pleasant, NJ). Effective cation exchange capacity (eCEC) was estimated as the sum of the base cations (K$_e$, Na$_e$, Ca$_e$, Mg$_e$) displaced with 1 M NH$_4$Cl (Peech et al., 1947) and Al extracted with 1 M KCl (Al$_K$; (Lin and Coleman, 1960). Different solutions were applied to assess Al and Fe distribution in the soil solid phase according to García-Rodeja et al. (2004). Briefly, total organo-metal (Al, Fe) complexes were estimated with 0.1 M Na-pyrophosphate solution (Al$_p$, Fe$_p$); whereas organo-metal (Al, Fe) complexes and inorganic non-crystalline Al and Fe oxyhydroxides were dissolved with 0.2 M ammonium oxalate-oxalic acid buffered at pH 3 in

the dark (Al_o, Fe_o). The total free Al pool was estimated with 0.5 M NaOH solution (Al_n) while total free Fe, including organo-Fe complexes, non-crystalline and crystalline Fe oxyhydroxides were estimated from an extraction with Na-dithionite-citrate (Fe_d) (Holmgren, 1967). Operatively-defined fractions of both metals were as follows: total free Al and Fe minus oxalate-extractable Al and Fe were considered an estimation of crystalline Al and Fe compounds (Al_c, Fe_c); oxalate-oxalic extracted Al and Fe minus Na-pyrophosphate extractable Al and Fe can be considered as an estimation of the inorganic non-crystalline Al and Fe compounds (Al_{ia}, Fe_{ia}). The organic-complexed Al pool was further characterized using 0.5 M $CuCl_2$ (Juo and Kamprath, 1979) and 0.33 M $LaCl_3$ (Hargrove and Thomas, 1981), resulting in Al_{Cu} and Al_{La}, respectively. Following García-Rodeja et al. (2004), these extractions allow differentiating operatively between high stability (Al_{oh}, as Al_p – Al_{Cu}), moderate stability (Al_{om}, Al_{Cu} – Al_{La}) and low stability (Al_{ol}, Al_{La} – Al_K) Al-humus complexes. For the determination of C in Na-pyrophosphate extracts (C_p), they were previously filtered by 0.45 μm-pore size fiberglass membranes to remove suspended particles. Afterwards, 10 mL of the extract were transferred to a flask and allow to dry completely in an oven at 40°. The dry extract was redissolved in 10 mL of concentrated H_2SO_4 and then, the released C was oxidized in excess with 1.8 N $Cr_2O_7K_2$ solution at 105 °C. After cooling, the extract was transferred to a volumetric flask and ended up with distilled water. The excess of $Cr_2O_7K_2$ in a sample aliquot is backtitrated with 0.1 N $(NH_4)_2Fe(SO_4)_2$ solution (Mohŕs salt) in the presence of few drops (2–3) of concentrated acids (H_2SO_4 and H_3PO_4) and 1% diphenylamine solution. Flame atomic absorption/emission spectroscopy was used for determining the concentrations of the different cations in the extracts.

The mineralogical characterization was carried out in the fine sand (50–100 μm) and clay fractions (<2 μm) of some illuvial horizons from soils P.2, P.21 and P.25. In order to minimize interferences during X-ray diffraction analysis, fine sand and clay samples were firstly treated with a 6%–H_2O_2 solution to remove soil organic matter and, subsequently, with a 2 M HCl solution to dissolve non-crystalline materials. Afterward, dry samples were finely ground. Minerals occurring in the analyzed samples were identified by using a Philips X-ray diffractometer (a PW1732 generator, a PW 1050 goniometer and a PW 1710 control unit with the PC-APD software v. 3.6B). X-ray diffraction patterns were obtained for non-treated sand and clay-sized samples, as well as clay-sized samples saturated with 0.5 M $MgCl_2$ solution (and in some cases with 1 M KCl solution), samples solvated with ethylene glycol, and after exposition to heating at 350° and 550 °C. Scanning was performed in the angle region 2-45° 2θ using a Cu Kα radiation (40 V, 30 mA), with a scanning speed of 0.02° 2θ (2 s counting time) or, in the case of analyses more in detail, scanning speed of 0.004° 2θ s^{-1} (5 s counting time). The obtained X-ray diffractograms were interpreted using the software MacDiff v. 4.2.5.

2.4. Total Hg determination

Total Hg concentration (Hg_T) was measured by atomic absorption spectroscopy after thermal combustion with a DMA-80 mercury analyzer (Milestone), using 80–100 mg of soil finely milled in an automatic agate mortar (Retsch RM100, Retsch RM200). The limit of detection (LOD) for Hg_T was 0.43 μg kg^{-1}, considering an average mass sample of 100 mg. In terms of precision of the method, all soil samples were analyzed in duplicate and reanalyzed when the coefficient of variation between replicates exceeded 10%. For accuracy and quality purposes (QA/QC), standard reference materials NCS DC 87,101 (soil, 14 ± 5 μg kg^{-1}) and GBW 07,427 (soil, 52 ± 6 μg kg^{-1}) were measured at the beginning of each analytical run and repeated every fifteen samples. The percentages of recovery were 96% for NCS DC 87,101 (average 13.5 $\pm$ 2.7 μg kg^{-1}, n = 9) and 98% for GBW 07,427 (average 50.7 $\pm$ 7.4 μg kg^{-1}, n = 9).

2.5. Statistical data treatment and calculations

Mercury enrichment factor (EF_{Hg}) was used, following Guédron et al. (2006), as a tool to discriminate the main source of Hg in soils distinguishing among an exogenic origin (i.e., from atmospheric inputs) or a lithological origin. Zirconium, whose total content was determined by an X-ray fluorescence analyzer (Siemens SRS3000), was used as a "conservative element" for EF_{Hg} calculation according to Eq. (1). The detection limit for Zr was 2 mg kg^{-1} and the working range was from 40 to 690 mg kg^{-1}.

$$EF_{Hg} = \frac{[Hg_{THor}]/[Zr_{Hor}]}{[Hg_{THorC}]/[Zr_{HorC}]} \tag{1}$$

where the subscript *Hor* refers to a given soil horizon and *Hor C* refers to the deepest soil sample collected in the C horizon of each soil. The brackets indicate concentration in mg kg^{-1} (for Zr) and μg kg^{-1} (for Hg). This approach assumes that Hg in the C horizon comes completely from a lithogenic origin. As much as EF_{Hg} values separate from 1, more predominant is the atmosphere as Hg source independently of the natural or anthropogenic origin. On the contrary, EF_{Hg} values close, or below 1, denote a predominant lithological origin.

A principal component analysis (PCA) was carried out to reduce the dimensionality of the database and summarize the variability in a few components (PCs). Varimax rotation was used because it maximizes the loadings of the variables on the extracted components. As the extracted principal components are orthogonal (i.e. independent), they are not subject to redundancy. Variables with loadings higher than 0.50 were considered relevant for each component (Abdi and Williams, 2010).

In order to model how soil parameters are involved in the Hg patterns observed in the soils studied, principal components regression (PCR) was performed, that is to say, a stepwise linear regression using the principal component scores obtained in PCA as predictor variables and Hg as the dependent variable. The suitability of the obtained model was tested by representing the values of predicted vs observed Hg. The weight of each principal component (wPC) was obtained by multiplying the score of each component by the corresponding standardized regression coefficient for each sample (Liu et al., 2003).

Relationships between Hg and soil properties were obtained following a Spearman rank correlation (r_s) considering that most of the results did not follow a normal distribution. The results of the statistical test were considered significant when p < 0.05. All statistical analyses were done using SPSS version 25.0 software for Windows.

3. Results and discussion

3.1. Physico-chemical and mineralogical soil properties

The morphology of all the studied soils is highly compatible with the traditional Podzol morphology (Mokma et al., 2004), showing thick and coarse-textured light-colored horizons (up to 125 cm in soil P.21) overlying horizons with darker colours, from blackish to reddish, presumably depending on the different degree of accumulation of organic matter and secondary Al and Fe compounds. Darker subsurface horizons do not show evidence of cementation whereas some soils present sub-horizons AE or EB. However, sometimes the morphological soil characteristics could not meet successfully all the chemical criteria for albic material and spodic horizon required by the World Reference Base for Soil Resources (WRB). As the classification of the studied soils is beyond the aims of this research, readers are referred to Monteiro et al. (2015) for detailed information about this issue.

The physico-chemical characteristics of the studied soils seem to be consistent with the podzolization as the main pedogenetic process that has been occurring in them. The extremely coarse texture of the studied soils, facilitating water infiltration, and forest vegetation dominated by *Pinus pinaster*, supplying litterfall characterized by low decomposition rate and high organic acid production, are well-known factors favoring

Table 1
Main physico-chemical characteristics of the studied soils as average values per type of horizon.

Hor	n	Sand	Silt	Clay	pH$_w$[a]	pH$_K$	C[b]	C$_p$	N	C/N	BS[c]	eCEC
							g kg^{-1}				cmol$_c$ kg^{-1}	
A	15	96.3 ± 2.2	2.5 ± 1.6	1.2 ± 1.1	4.7 ± 0.6	3.2 ± 0.5	18.1 ± 10.2	2.9 ± 2.9	0.5 ± 0.3	40 ± 13	2.4 ± 1.4	2.5 ± 1.4
E	17	98.8 ± 0.7	0.8 ± 0.7	0.5 ± 0.4	5.0 ± 0.3	3.7 ± 0.3	1.0 ± 0.9	0.1 ± 0.3	0.0 ± 0.0	37 ± 21	1.0 ± 0.1	1.1 ± 0.1
Bh/Bs	20	97.5 ± 2.2	1.1 ± 1.0	1.4 ± 1.3	5.0 ± 0.4	4.1 ± 0.3	7.4 ± 5.6	1.8 ± 2.8	0.2 ± 0.2	36 ± 13	1.1 ± 0.4	1.4 ± 0.5
C	15	97.0 ± 3.1	1.6 ± 2.2	1.4 ± 1.4	5.4 ± 0.3	4.4 ± 0.3	1.0 ± 0.9	0.3 ± 0.6	0.0 ± 0.0	5 ± 2	1.0 ± 0.3	1.1 ± 0.4

[a] pH$_w$ and pH$_k$ are pH values measured in distilled water and 0.1 M KCl. respectively.
[b] C. C$_p$. N: total carbon content. Na-pyrophosphate extractable C and total nitrogen content.
[c] BS: sum of base cations (Na, K, Ca, Mg); eCEC: effective Cation Exchange Capacity.

the podzolization (Lundström et al., 2000; Mokma et al., 2004; Valerio et al., 2016).

The main physico-chemical characteristics of the ten studied podzolic soils are shown, as mean values per genetic horizon, in Table 1. Data of the complete population of soil samples can be found in Supplementary Material (Table S1).

Particle-size distribution is dominated by the sand fraction (coarse + fine) whose average is above 90% for all horizons, although it is somewhat higher in the E horizons (mean 99%). Podzols with an extremely coarse-textured as those of the present study, with sand contents above 90%, are common in coastal and inland dune areas worldwide (Skjemstad et al., 1992; Sauer et al., 2008; Cornelis et al., 2014; Jankowski, 2014; Krettek et al., 2020). It must be remembered that coarse textures favor water percolation, which contributes to the mobilization (translocation) of soluble organic matter and associated metals (Schaetzl et al., 2015). The predominance of the sand fraction, although somewhat lower than for Podzols in coastal areas, is also recurrent in Podzols from mountains areas in central and south Europe (Bonifacio et al., 2006; Waroszewski et al., 2013, 2015; Gómez-Armesto et al., 2021). The maximum silt contents are found in the A horizons (average 2.5 ± 1.6%), and the lowest in the E horizons (mean 0.8 ± 0.7%). The clay fraction is the least abundant particle size fraction in all soil profiles, with the highest content found in the illuvial (Bh, Bhs and Bs) and C horizons (up to 1.4%). Compared to the E horizons, the increase of the clay fraction in the illuvial horizons (Bh, Bhs and Bs) has been frequently observed in Podzols, being attributed to the accumulation of Al and Fe oxyhydroxides and organic C mobilized from overlying horizons due to podzolization (Sauer, et al., 2008; Cornelis et al., 2014).

Following this particle-size distribution, all soil samples show a sandy texture in agreement with the low content of weatherable minerals in the soil parent material (mostly quartz sands).

All the studied soils can be characterized from moderate to strongly acidic, with values of pH in distilled water (pH$_w$) increasing with soil depth from an average of 4.7 ± 0.6 in the A horizons to 5.4 ± 0.3 in the C horizons (Table 1). The increase of pH$_w$ with depth was also reported in Podzols from a nearby area in NW Spain (Ferro-Vázquez et al., 2014; Gómez-Armesto et al., 2021), along the Finnish coast (Mokma et al., 2004), in a Podzol from the north USA (Schaetzl et al., 2015) or in sandy podzolic soils from Poland (Waroszewski et al., 2013, 2015; Jankowski, 2014). As expected, the average values of the pH measured in saline solution (pH$_k$) were lower than pH$_w$, varying from 3.2 to 4.4 in the A and C horizons, respectively, but keeping the increasing trend with soil depth already observed for the pH$_w$. Our pH$_k$ values are in the range (2.7–5.3) observed for podzolic soils in Norway, Poland, Germany and Belgium (Sauer et al., 2008; Jankowski, 2014; Krettek et al., 2020). In general, the lowest values of pH in the A horizons could be associated with the organic acidity derived from the decomposition of litter, as it is denoted from the highest contents of organic C.

Mean values of total soil organic C (SOC), which is considered equivalent to total C due to the absence of inorganic carbonates, ranged from 18.1 g kg^{-1} in the A horizons to 1.0 g kg^{-1} in the C and E horizons (Table 1). SOC values showed an increase in the subsoil (average 7.4 g

kg^{-1}) that correspond to the illuvial horizons (Bh, Bs and Bhs). This bimodal distribution of SOC is characteristic of Podzols (Mokma and Buurman, 1982; Lundström et al., 2000), with E horizons almost depleted in C due to eluviation and accumulation of SOC in the illuvial layers. Recently, Rothstein et al. (2018) concluded that up to 80% of the dissolved organic C occurring in the B horizons of a pine forest soil came from the organic (O) horizon, without discarding the contribution of fine tree roots and the decomposing activity of microbial communities.

In general, SOC values in the studied soils are in the range (1–72 g kg^{-1}) observed for mineral horizons of Podzols and podzolic soils worldwide (Mokma et al., 2004; Ferro-Vázquez et al., 2014; Jankowski, 2014; Waroszeski et al., 2013, 2015; Rothstein et al., 2018; Krettek et al., 2020; Gómez-Armesto et al, 2021). Total contents of N are below the detection limit in most of the samples corresponding to C and E horizons, whereas an average of 0.5 and 0.2 g kg^{-1} was found for A and illuvial horizons, respectively (Table 1).

In Podzols and podzolic soils, together with the amount of organic matter, the quality of the organic matter also takes a key role. The degree of organic matter humification could affect the movement of water through the soil and, consequently, the vertical and lateral transport of solutes and colloids (Deurer et al., 2000, Jankowski, 2014) and the own intensity of the podzolization process. The C/N ratio, an indirect estimation of the degree of humification of soil organic matter, shows considerably higher mean values in the A, E and illuvial horizons (where it ranged from 36 to 40) compared to the C horizons (Table 1). Moreover, the C/N ratios in the present work are well above those showed in previous studies with similar soils where they varied from 12 to 30 (Jankowski, 2014; Krettek et al., 2020), and they did not show a diminution trend from the A to the illuvial horizons as often reported in Podzols (Jankowski, 2014; Krettek et al., 2020). The observed high values of the C/N ratios could be due to the low content of total N, which is common in the litterfall from coniferous species (McGroddy et al., 2004), but they also suggest a lower rate of organic matter humification (Grand and Lavkulich, 2011). The scarce transformation of the organic matter in the studied soils is consistent with the high lignin and low N content in pine needles that slow down its mineralization (Krishna and Mohan, 2017). Our low total N values are in line with Rothstein et al. (2018), who reported an abundance of lignin-derived compounds and low levels of protein and other N-bearing compounds in the dissolved organic matter from organic horizons of pine forests. The low values of the Na-pyrophosphate extractable C (C$_p$), which can be also considered as an estimation of the well-humified soil organic C, support a relatively low organic carbon mineralization. The values of C$_p$ in the A and Bh/Bs horizons averaged 2.9 and 1.8 g kg^{-1} respectively, whereas in the E and C horizons C$_p$ is almost absent (Table 1). Moreover, the low values of the C$_p$/C molar ratio (0.2–0.3) also point out that only a small fraction of the total organic matter in the A and Bh/Bs horizons can be considered well-humified.

The effective cation exchange capacity (eCEC) is very low in all horizons (<2.5 cmol$_c$ kg^{-1}) with the cation exchange complex dominated by base cations (mostly Ca) whereas exchangeable Al mean values were below 0.3 cmol$_c$ kg^{-1} (Table 1, Table S1). This unexpected result, taking into account the strong acidity of the studied soils and the poverty

Table 2
Distribution of Al and Fe compounds in the soil solid phase, total Hg concentrations and enrichment factor as average values per type of horizon.

Hor	n	Al_p [a]	Al_o	Al_n	Fe_p	Fe_o	Fe_d	Al_p/Al_o	Al_o/Al_n	Fe_p/Fe_o	Fe_o/Fe_d	Hg_T [b]	EF_{Hg} [c]
		g kg^{-1}										μg kg^{-1}	
A	15	0.3 ± 0.2	0.2 ± 0.2	0.3 ± 0.3	0.1 ± 0.1	0.1 ± 0.1	0.3 ± 0.2	1.1 ± 0.1	0.8 ± 0.2	0.7 ± 0.1	0.5 ± 0.2	11.9 ± 6.2	2.8 ± 2.3
E	17	0.2 ± 0.0	0.2 ± 0.0	0.2 ± 0.1	0.0 ± 0.1	0.1 ± 0.1	0.2 ± 0.2	1.0 ± 0.0	1.0 ± 0.1	0.7 ± 0.4	0.3 ± 0.1	4.3 ± 1.4	0.9 ± 0.4
Bh/ Bs	20	1.2 ± 0.8	1.8 ± 1.6	2.7 ± 2.2	0.4 ± 0.7	0.4 ± 0.5	0.8 ± 0.9	0.8 ± 0.3	0.7 ± 0.1	0.8 ± 0.3	0.5 ± 0.2	9.8 ± 4.7	1.7 ± 1.0
C	15	0.5 ± 0.3	0.7 ± 0.5	1.5 ± 1.1	0.1 ± 0.2	0.1 ± 0.2	0.5 ± 0.8	0.7 ± 0.2	0.6 ± 0.2	0.8 ± 0.1	0.4 ± 0.1	7.0 ± 3.3	1.2 ± 0.8

[a] Al_p (Fe_p), Al_o (Fe_o), Al_n and Fe_d: Al (Fe) extracted with Na-pyrophosphate (p), ammonium oxalate-oxalic acid (o), Al extracted with Na hydroxide (n) and Fe extracted with Na-dithionite-citrate (d), respectively

[b] Hg_T: Total Hg content.

[c] EF_{Hg}: enrichment factor of Hg estimated taking into account the Zr content of the C horizon of each profile.

in base cations of the parent material (mostly quartz sands), contrasts with previous studies reporting Al as the dominant cation in the cation exchange complex of Podzols (Waroszeswki et al., 2013; Valerio et al., 2016). Despite this, our values of eCEC are in the range reported by Różański et al. (2016) for an Albic Podzol (1.4–5.5 cmol$_c$ kg^{-1}).

The mineralogical composition of the fine sand is almost identical in the three samples (Table S2), with quartz as the dominant mineral (>90%) accompanied by minor amounts (2–5%) of K-feldspar (microcline) and plagioclase (albite). Traces of muscovite were also observed in the sample of the soil P.25. The great abundance of quartz in the sand fraction is consistent with the extremely coarse texture observed in the studied soils. Regarding the mineralogical composition of the clay fraction, it is also dominated by quartz with microcline as the second most abundant mineral in all samples (2–5%). However, in the clay-sized fraction albite occurred in lower amounts than in the sand fraction, being < 2% in weight or lower (traces) in the assessed illuvial horizons (Table S2). The presence of pedogenetic clay minerals is only represented by traces of illite in all samples and kaolinite in the illuvial horizons of the soils P.2 and P.21.

The mineralogical composition observed in the sand and clay-size fractions was in agreement with that reported by Mokma et al. (2004) for Podzols in Finland developed from sandy parent materials, where quartz dominates the clay fraction with only very low amounts of illite, chlorite and illite-vermiculite. Recently, Cornelis et al. (2014) also observed dominance of quartz in the clay fraction of Podzols developed from a similar parent material (beach sand), whereas the pedogenetic clay minerals they found were illite, kaolinite and chlorite, similar to the current study. The occurrence of pedogenetic clay minerals (illite and kaolinite) in the illuvial horizons of the soils P.2, P.21 and P.25 can be interpreted, following Cornelis et al. (2014), as a result of the dissolution of primary minerals due to podzolization.

3.2. Contents and distribution of secondary al and Fe compounds

Secondary Al and Fe compounds, including metal (Al, Fe)-humus complexes and Al and Fe oxyhydroxides with different degree of crystallinity, play a key role in several soil functions and their vertical distribution becomes a distinctive feature in Podzols (Buurman and Jongmans, 2005; Sauer et al., 2007; Ferro-Vázquez et al., 2014, 2020).

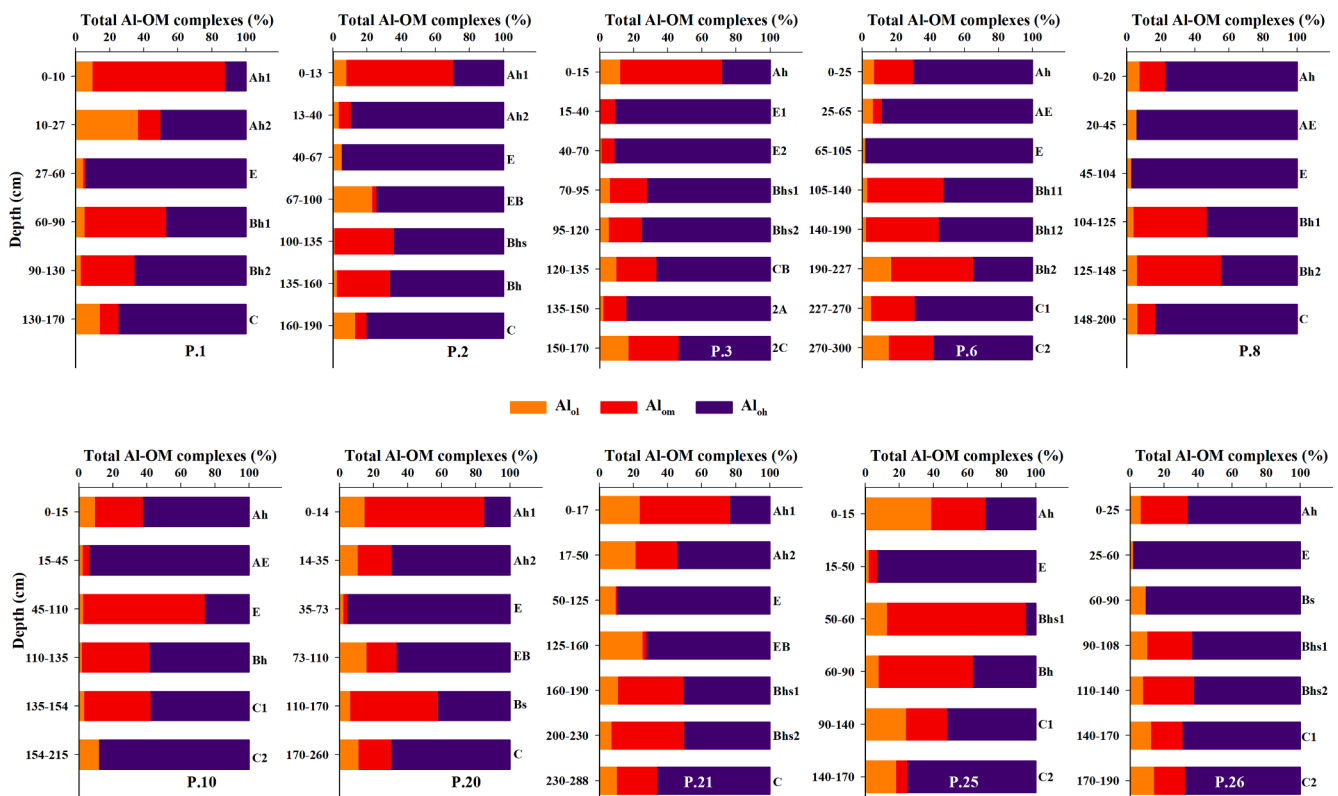Although a recent study highlights several uncertainties about the

Fig. 1. Percentage of organically complexed Al distributed in complexes of low, moderate and high stability (Al_{ol}, Al_{om}, Al_{oh}) in the studied soils.

use of selective dissolution extractions to define secondary Al and Fe compounds in soils (Rennert, 2019), their application still results reasonably for a wide variety of soils including Podzols (Parfitt and Childs, 1988).

The contents of extractable secondary Al and Fe compounds of the studied soils are shown in Table 2 (as an average for each genetic horizon), whereas the absolute values for all samples can be found in Table S1.

All the chemical extractions assessed (NaOH, ammonium oxalate-oxalic acid and Na-pyrophosphate) showed Al values with a similar trend with soil depth. The lower mean values of Al are found in the A and E horizons ($0.2–0.3$ g kg^{-1}) and the highest in the illuvial layers ($1.2–2.7$ g kg^{-1}), whereas the C horizons present intermediate mean values ($0.5–1.5$ g kg^{-1}).

The similar contents of NaOH-extractable Al (Al$_n$) and ammonium oxalate-oxalic acid-extractable Al (Al$_o$) (Table 2), indicate that secondary crystalline Al compounds do not occur in significant amounts in the A and E horizons. However, Al$_o$/Al$_n$ ratios for the illuvial (Bh, Bs) and C horizons (0.7 and 0.6, respectively) suggest that secondary crystalline Al compounds represent a meaningful fraction (approximately 30–40%) of their total free Al pool. The similarity of Al$_p$ and Al$_o$ mean values in the A and E horizons ($0.2–0.3$ g kg^{-1}) indicates that inorganic non-crystalline Al compounds are scarce in these horizons (Al$_p$/Al$_o$ ratios ≈ 1, Table 2). On the contrary, they contribute to some extent to the total free Al pool of the illuvial horizons, particularly in the soils P.6, P.8, P.10, P.20 and P.26 where Al$_o$ > Al$_p$ (Table S1).

Aluminum fractionation is widely dominated by Na-pyrophosphate extractable Al (Al$_p$) which, despite some uncertainties about its specificity (Kaiser and Zech, 1996; Rennert, 2019), should be interpreted as a useful estimation of the organically complexed Al in Podzols and podzolic soils (Highasi, 1983; Mokma et al., 2004; Kaal et al., 2008; Grand and Lavkulich, 2011; Schaetzl et al., 2015). The prevalence of the organically-complexed Al (Al$_p$) in the studied soils is supported by the Al$_p$/Al$_o$ ratios ≈ 1 in the A and E horizons, as well as values above 0.7 in the illuvial and C horizons (Table 2). The values of Al$_p$ in the soils of the current study varied between 0.2 and 2.5 g kg^{-1}, being in the range $0.1–20$ g kg^{-1} reported for Al$_p$ in Podzols and podzolic soils from boreal and temperate areas worldwide (Mokma et al., 2004; Kaal et al., 2008; Sauer et al., 2008; Grand and Lavkulich, 2011; Ferro-Vázquez et al., 2014; Peña-Rodríguez et al., 2014; Schaetzl and Rothstein, 2016; Valerio et al., 2016; Gómez-Armesto et al., 2021). The concomitant occurrence of peaks of Na-pyrophosphate extractable Al and SOC in the illuvial Bh and Bhs horizons can be considered as evidence for Al and organic C mobilization from overlying horizons, which manifested a considerable depletion of these soil compounds.

Aluminum-organic matter associations have been characterized in Podzols to go further in the role of Al fractionation in pedogenetic and environmental issues (Coelho et al., 2010; Ferro-Vázquez, et al., 2014, 2017, 2020; Gómez-Armesto et al., 2021). In the current study, the Al-OM complexes follow the next sequence in order of abundance in all horizons: high stability Al-OM complexes (Al$_{oh}$) > moderate stability Al-OM complexes (Al$_{om}$) > low stability Al-OM complexes (Al$_{ol}$).

The Al$_{oh}$ complexes (range $0.2–14.6$ cmol$_c$ kg^{-1}; Table S1) show the highest values in the illuvial horizons (Bh, Bhs, Bs) where they account for a mean of 54% of the total Al-OM complexes in these horizons. The Al$_{oh}$ complexes averaged 85 and 51% of total Al-OM complexes for the E and A horizons, respectively (Fig. 1). Inaccuracies due to the very low values of extractable Al could satisfy the high percentage of Al$_{oh}$ in the E horizons (Ferro-Vázquez et al., 2014), whereas poorly-humified organic matter (mean C/N ≈ 40, Table 1) contributed to the occurrence of unsaturated metal–organic C complexes in the A horizons (Schaetzl and Rothstein, 2016).

The moderate stability Al-OM complexes (Al$_{om}$) in all samples varied from their almost absence in some E horizons to the highest values (13.4 cmol$_c$ kg^{-1}) in the illuvial Bh horizon of the soil P.25. These complexes were the most abundant Al-OM association in the uppermost horizons of

soils P.1, P.2, P.3, P.20 and P.21 (with values close to 2 cmol$_c$ kg^{-1}), being quantitatively similar to Al$_{oh}$ in the illuvial horizons of the soils P.1, P.6, P.8, P.20, P.21 and P.25 (Table S1). On average, the low stability Al-OM complexes (Al$_{ol}$) account for<10% of the total Al-OM complexes (Table S1, Fig. 1). Despite their lower values, the Al$_{ol}$ complexes are relevant in terms of podzolization because their greater solubility could favor their downward migration (Ferro-Vázquez et al., 2014).

Regardless of the chemical extraction, the mean content of secondary Fe compounds was lower than secondary Al compounds per genetic horizon (Table 2), which is consistent with the extremely low contents of Fe in the soil parent material (quartz sands).

The vertical distribution of secondary Fe compounds follows that for Al, with the lower mean values (<0.3 g kg^{-1}) in the A and E horizons and the highest (up to < 0.8 g kg^{-1}) in the illuvial horizons (Table 2). The Na-pyrophosphate extractable Fe (Fe$_p$), which is considered an estimate of the organic matter-complexed Fe (McKeague, 1967), ranged from below the detection limit up to 3.1 g kg^{-1} (Table S1). The Fe$_p$ values obtained in this study were similar to the range ($0.1–8.0$ g kg^{-1}) found in Podzols developed from sandy parent materials (Mokma et al., 2004; Sauer et al., 2008; Grand and Lavkulich, 2011; Schaetzl and Rothstein, 2016). The mean values of the Fe$_p$/Fe$_o$ ratio, above 0.7 in all horizons, suggest that most of the non-crystalline and short-range ordered Fe (resulted from ammonium oxalate-oxalic acid extractable Fe, Fe$_o$) are complexed by soil organic C as reported by previous studies (Sauer et al., 2008; Ferro-Vázquez et al., 2014). However, this interpretation should be done with caution as extractions carried out at pH ≥ 7 (as the Na-pyrophosphate) can release Fe from oxyhydroxides in E and illuvial horizons of Podzols (Neubauer et al., 2013; Regelink et al., 2014). However, the significant positive correlation between Fe$_p$ and total organic C ($r_s = 0.557$; $p = 0.000$; $n = 52$), supports the previous consideration about the nature of Fe released after Na-pyrophosphate extraction.

Mean values of total free Fe compounds in non-silicate forms (Fe$_d$) varied from 0.2 to 0.8 g kg^{-1} depending on the genetic soil horizon (Table 2), with a notable accumulation in the illuvial horizons as commonly occurs in Podzols (Ferro-Vázquez et al., 2014; Schaetzl and Rothstein, 2016; Krettek et al., 2020; Gómez-Armesto et al., 2021). Following the Fe$_o$/Fe$_d$ ratios, secondary crystalline Fe compounds (Fe$_c$, estimated as Fe$_d$ – Fe$_o$) are the most abundant Fe fraction in all horizons unless for the illuvial ones, where Fe is evenly distributed between organically-complexed Fe and crystalline Fe compounds (50% each). The greater occurrence of crystalline Fe compounds observed in the A and E horizons is consistent with podzolization, which will remove from these horizons those more easily soluble Fe compounds (organically complexed Fe and Fe in short-range ordered minerals) favoring preservation of less soluble crystalline Fe compounds.

The vertical distribution of secondary Al and Fe compounds, mainly characterized by an impoverishment of secondary Al and Fe compounds in A and E horizons and a predominance of metal (Al, Fe)-organic matter associations in the illuvial horizons, is consistent with the podzolization as the main pedogenetic process characterizing the studied soils. The downward translocation of Al and Fe compounds, as well as organic matter, is a common feature recognized in Podzols (Lundström et al., 2000; Buurman and Jongmans, 2005; Sauer et al., 2007). The accumulation of metal (Al, Fe)-organic matter associations in illuvial horizons could occur due to their previous mobilization as particles or in the soil solution (Tolpeshta and Sokolova, 2009; Schaetzl and Rothstein, 2016). Afterwards, the immobilization of metal–organic matter associations in the illuvial horizons could take place due to an oversaturation of the organic C complexation capacity (Nierop et al., 2002; Jansen et al., 2005), forming coatings on inorganic particles (Yuan et al., 1998; Eusterhues et al., 2007; Krettek et al., 2020) or adsorbed onto secondary minerals (Eusterhues et al., 2005; Spielvogel et al., 2008). In the study area, the nature of the soil parent material (nutrient-poor and prone to develop coarse-textured soils) as well as coniferous dominant vegetation
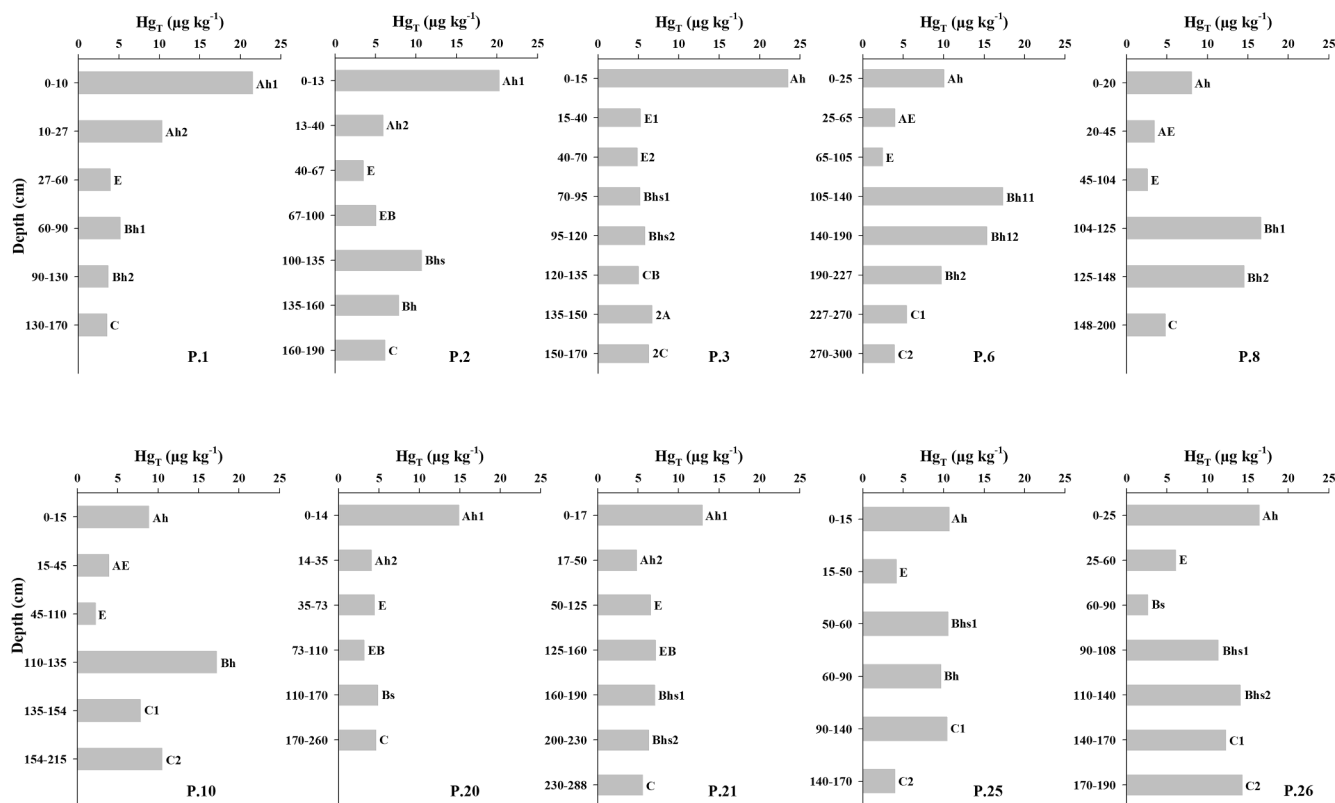
Fig. 2. Total Hg concentration (Hg$_T$) in the studied soils on a horizons basis.

prone to abundant organic acid production, would favor soil podzolization.

3.3. Total Hg contents and their vertical distribution patterns

All the studied soils have very low total Hg contents (Hg$_T$), which range from 2.2 to 23.5 µg kg^{-1} (Fig. 2, Table S1). On a genetic horizon basis (Table 2), mean Hg$_T$ values decrease from the A horizons (11.9 ± 6.2 µg kg^{-1}) to the E horizons (4.3 ± 1.4 µg kg^{-1}), then increase in the illuvial horizons (9.8 ± 4.7 µg kg^{-1}) and diminish again until the deepest soil layers (C horizons, 7.0 ± 3.3 µg kg^{-1}). Total Hg levels in the studied soils are well below the threshold of 100 µg kg^{-1} suggested as indicative for Hg non-contaminated soils (Xin and Gustin, 2007). In this sense, it can be considered that the studied soils are not influenced by any point source of Hg emissions. This is also supported by the relatively low average (<3, Table 2) of the Hg enrichment factor (EF$_{Hg}$), being necessary levels > 10 to consider a significant Hg contamination (Hissler and Probst, 2006; Guédron et al., 2006; Klaminder et al., 2008).

The levels of Hg$_T$ in the soils of the Leiria National Forest are in the same order as pristine Podzols worldwide, where mean Hg levels in mineral horizons scarcely exceed 50 µg kg^{-1} (Do Valle et al., 2005; Richardson et al., 2013; Yu et al., 2014; Różański et al, 2016; Gruba et al., 2019; Nave et al., 2019; Gómez-Armesto et al., 2020b, 2021). Low values of Hg$_T$ are also found in the mineral horizons of other pristine soil types such as Ferralsols (Do Valle et al., 2005; Guédron et al., 2006; Grimaldi et al., 2008; Fiorentino et al., 2011), Acrisols (Guédron et al., 2006, 2009), Ultisols (Grimaldi et al., 2008), Andosols (Peña-Rodríguez et al., 2012) and brown-earth forest soils (Zhou et al., 2017).

A thorough examination of Hg$_T$ with depth in the studied soils revealed some distinctive features that allow us to identify three different patterns of Hg$_T$ according to the occurrence of their maximum values (Fig. 2). The pattern I is characterized by the occurrence of the greatest Hg$_T$ values in the A horizons as in the soils P.1, P.2, P.3, P.20 and P.21, whereas a secondary peak is found in the illuvial horizons (as

in soil P.2). Contrarily, the pattern II is featured by the greatest values of Hg$_T$ in the illuvial horizons (soils P.6, P.8 and P.10) whereas slightly lower levels occurred in the Ah horizons. Pattern III (depicted by the soils P.25 and P.26) is characterized by an even distribution of Hg$_T$ with soil depth without a distinctive maximum of Hg$_T$ neither in the Ah nor in the illuvial horizons.

The soils with the pattern I are consistent with the typical trend found for forest soils where Hg$_T$ distribution resembles that of the organic C content (Yu et al., 2014; Du et al., 2019; Gruba et al., 2019). This is supported by the strong correlation between total organic C and Hg$_T$ in the A horizons (r$_s$ = 0.807, p = 0.000, n = 15) which is similar to that reported for both parameters (r^2 = 0.90) by Nave et al. (2019) in Podzols from coastal areas. Total Hg peaks in the A horizons are presumably due to the transference of atmospheric Hg to the soil surface by dry, wet and litterfall deposition (Demers et al., 2007; Gong et al., 2014; Gerson et al., 2017; Gómez-Armesto et al., 2020c). The atmosphere as the main source of Hg$_T$ in the A horizons of the studied soils, is also confirmed by the fact that the highest values of the EF$_{Hg}$ were found in those surface horizons (Table 2). However, the lithogenic contribution by weathering to the Hg accumulated in the A horizons cannot be ruled out, but the low values of Hg$_T$ in the C horizons lead to consider the lithology as a minor relevant source for Hg$_T$ in the A horizons.

A greater content of Hg$_T$ in the illuvial horizons than in the upper-most mineral soil layers (pattern II) is often reported in the literature for Podzols and podzolic soils (Aastrup et al., 1991; Schwesig and Matzner, 2000; Dreher and Follmer, 2004; Hissler and Probst, 2006; Navrátil et al., 2009, 2016; Richardson et al., 2013; Gómez-Armesto et al., 2020b, 2021). For pattern III, no distinctive peaks of Hg$_T$ were found throughout the pedon, similar to that reported by Nave et al. (2019) for several Podzols located in the USA.

Different soil-forming factors, mostly soil age and podzolization intensity (Mokma et al., 2004; Sauer et al., 2008; Cornelis et al., 2014), led to a different distribution of organic C and secondary Al and Fe compounds among illuvial and eluvial soil layers that could explain, in some

extent, the differences between the three described Hg patterns. As organic C, Al and Fe compounds are mobilized downwards due to podzolization (Buurman and Jongmans, 2005; Schaetzl and Rothstein, 2016; Rothstein et al., 2018), it would be expected that these compounds could behave as carrier phases transferring Hg to deeper soil layers (Hissler and Probst, 2006; Jiskra et al., 2015). In any case, all the patterns described for Hg_T in the Leiria soils showed their lower values in the E horizons, which is consistent with the effect of podzolization removing most of the geochemically reactive soil components in these soil layers. However, the narrow association between Al and Fe compounds and Hg is not exclusive of Podzols, as it was also found for Ferralsols and Acrisols (Guédron et al., 2009).

Considering that the lithology (through the weathering of soil parent material) scarcely contributes to the Hg accumulation in the illuvial horizons compared to atmospheric sources, it is interesting to trace how Hg can be mobilized from overlying horizons. Several features of the studied soils point out that Hg is likely mobilized towards illuvial horizons in combination with soluble or colloidal organic C. The predominance of organic matter-metal associations in the A horizons with a low metal–organic C saturation facilitates their downward migration (Jansen et al., 2005; Schaetzl and Rothstein, 2016). The latest findings from field studies in Podzols can help to support the key role of organic matter in Hg mobilization. Schaetzl and Rothstein (2016) showed that soluble organic matter becomes a relevant carrier phase of metals in coarse-textured Podzols, such Al and Fe, but also Hg as it was aforementioned. Recently, Rothstein et al. (2018) indicated that a high degree of C saturation in the E horizons would allow the migration of unaltered C from the surface to the illuvial horizons. The mean value of the Al_p/C_p atomic ratio of the E horizons indicated highly saturated organic C (0.20) and thus, in agreement with Rothstein et al. (2018), a fraction of Hg trapped by organic matter in the A horizons could reach directly the illuvial horizons being part of decomposed organic matter debris. This is consistent with previous studies that indicate Hg mobilization is preferentially associated with partially degraded organic matter (Dmytriw et al., 1995; Guédron et al., 2009). In definitive, it should be reasonable to think that organic matter (either as dissolved C or complexed with metals) is involved in the downwards Hg migration in Leiria soils following one or several of the mechanisms abovementioned. The role of organic C in downwards Hg mobilization, transported either bound to dissolved organic C or as part of the clay-humic complex (Dreher and Follmer, 2004), was also reported in Podzols located worldwide (Do Valle et al., 2005; Hissler and Probst, 2006; Navrátil et al., 2009; Blackwell et al., 2014).

According to Schlüter (1996), two different (but not self-exclusive) mechanisms involving dissolved organic matter (DOM) could account for the Hg accumulation we observed in the illuvial horizons. In the first one, it is proposed that DOM acts as a bridge between inorganic Hg^{2+} species leached in soil solution and secondary Al and Fe compounds occurring in the illuvial horizons. Thus, DOM is initially adsorbed by secondary Al and Fe compounds in the illuvial horizons, being afterward available to retain the Hg^{2+} species leached in soil solution. A second mechanism, probably the dominant, can take place when Hg is mobilized as DOM-metal(Al, Fe, Hg) complexes and then immobilized in the illuvial horizons through adsorption to secondary Al and Fe oxyhydroxides (Eusterhues et al., 2005; Spielvogel et al., 2008). In the illuvial horizons of the soils from Leiria National Forest, characterized by a dominance of organic matter-metal(Al, Fe) associations with high metal/C atomic ratios that promote their immobilization (Nierop et al., 2002; Jansen et al., 2005), the precipitation of DOM-metal complexes is the more likely process responsible for Hg accumulation in these horizons.

However, Hg retention as part of the organic C-rich coatings formed on inorganic particles (Yuan et al., 1998; Eusterhues et al., 2007; Krettek et al., 2020) or adsorbed by secondary clay minerals such as kaolinite (Sarkar et al., 2000) cannot be discarded. This mechanism is expected to contribute scarcely to Hg retention in the illuvial horizons of Leiria soils
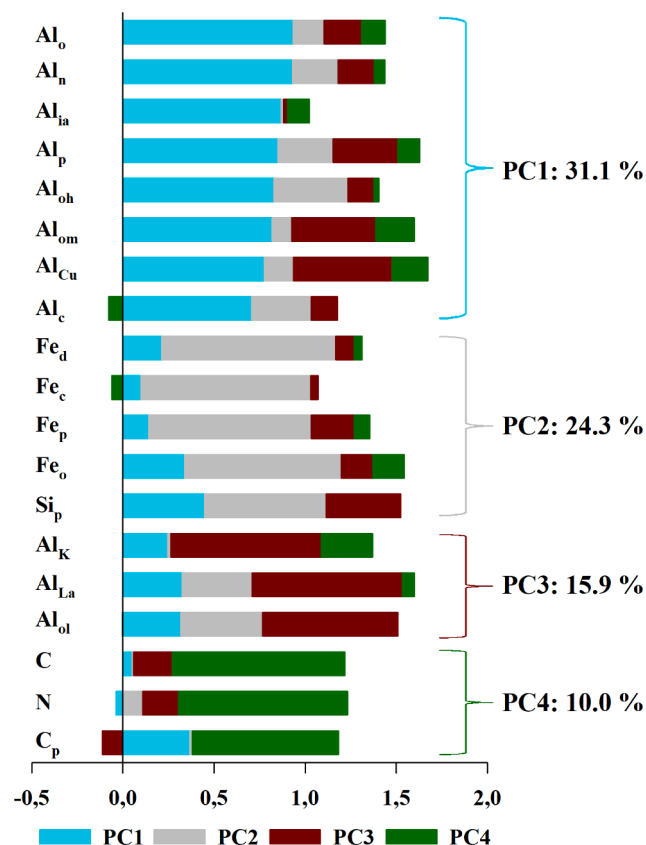

Fig. 3. Loadings of each variable included in the principal component analysis for each principal component (PC) obtained.

considering the very low contents of secondary Al and Fe compounds (Table S1), and the trace amounts of kaolinite (Table S2) which, at the mean pH of illuvial soils (5.0), their Hg adsorption capacity is considerably diminished (Sarkar et al., 2000).

3.4. Role of soil compounds in the Hg distribution

An exploratory non-parametric correlation analysis revealed interesting correlations between Hg_T and different soil parameters in the studied Podzols (Table S3). For example, Hg_T was strongly correlated to total organic C ($r_s = 0.722$, $p = 0.000$, $n = 67$), to a fraction of the organic matter-Al associations estimated by $CuCl_2$ extraction ($r_s = 0.617$, $p = 0.000$, $n = 67$), and to non-crystalline Fe compounds (Fe_o, $r_s = 0.617$, $p = 0.000$, $n = 67$). These correlations were consistent with the relevance given to these soil compounds in studies about Hg in Podzols and podzolic soils (Schwesig and Matzner, 2000; Hissler and Probst, 2006; Navrátil, et al. 2009; Richardson et al. 2013; Peña-Rodríguez et al., 2014; Nave et al., 2019; Gómez-Armesto et al., 2020b, 2021).

The PCA analysis, made to go further on the soil components and processes that could explain Hg distribution in the studied soils, extracted four components (eigenvalues > 1) which together accounted for 88.4% of the soil properties variance (Fig. 3 and Table S4). The components PC1 and PC2 showed the largest percentages of variance explained (34.1 and 24.3%, respectively). PC1 is mainly associated with different Al compounds that could occur in soils, including medium and high stability Al-humus complexes (Al_{Cu}, Al_{om}, Al_{oh}, Al_p), oxalate and NaOH-extracted Al (Al_o and Al_n) as well as inorganic crystalline and non-crystalline Al forms (Al_c and Al_{ia}). PC2 includes variables related to Fe compounds (Fe_p, Fe_o, Fe_d, Fe_c) and Na-pyrophosphate-extracted Si (Si_p). PC3, which explained 15.9% of the variation of the soil data, is mainly related to exchangeable Al (Al_K) and low stability Al-humus complexes (Al_{La}, Al_{ol}). Finally, PC4 accounted for 14.0% of the
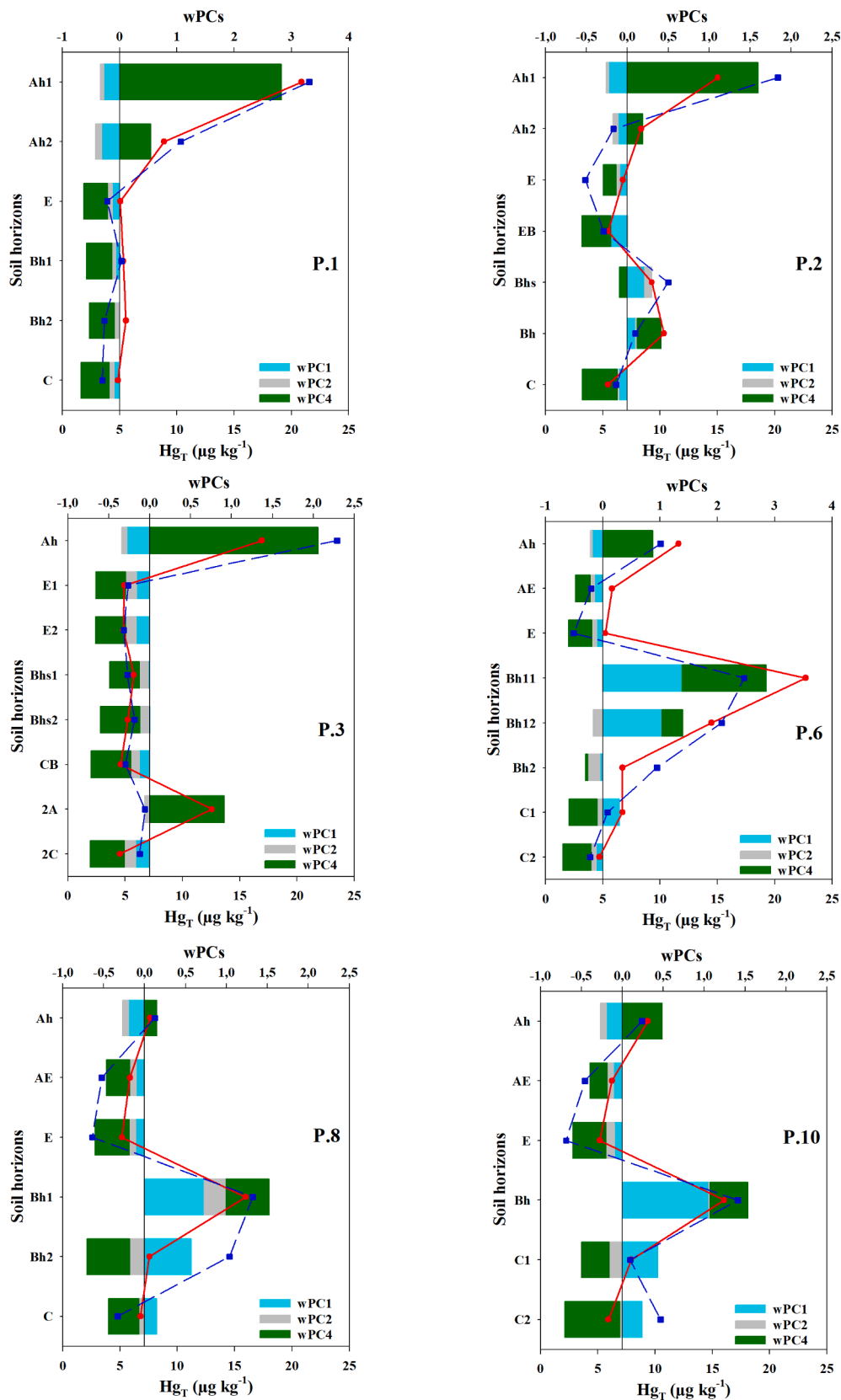
Fig. 4. Contribution of each PC included in the PCR (wPCs) to the total Hg prediction on a horizon basis. Red dotted and blue dashed lines represent predicted and observed Hg$_T$, respectively.
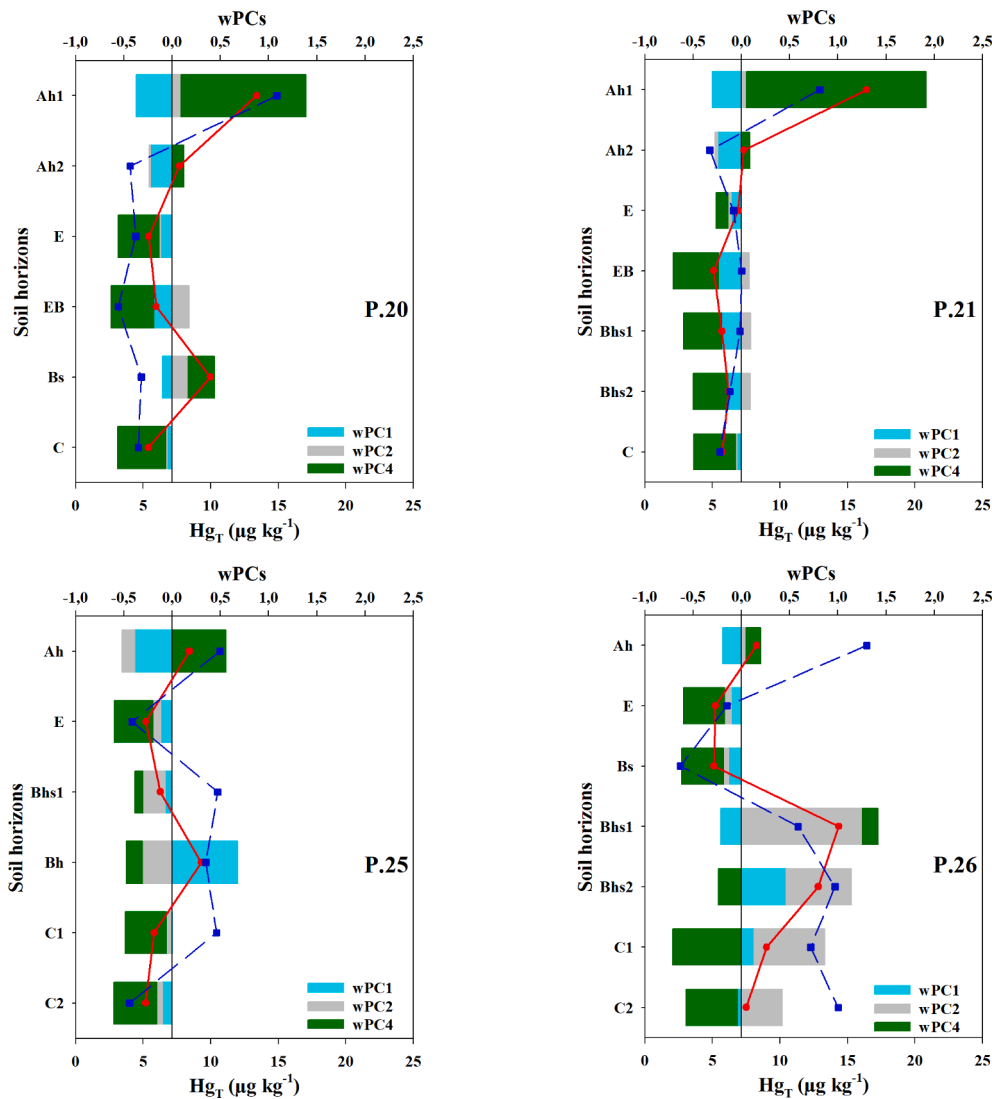
Fig. 4. (*continued*).

variance and it involved variables related to soil organic matter of different degree of humification (C, N, C$_p$). The results of the PCA confirmed our aforementioned assumption about organic C and Al and Fe compounds as main carrier phases responsible for both Hg mobilization and accumulation in the soils of the Leiria National Forest.

A principal component regression analysis (PCR), i.e. a stepwise linear regression analysis using the scores of the four PCs as new variables, was performed to predict the total Hg content (Hg$_{Tp}$) of each horizon. The resulted model included PC4, PC1 and PC2 as predictor variables obtaining an adjusted R^2 of 0.652 (Eq. (2)).

$$Hg_{Tp} = 8.24 + 3.58 * PC4 + 1.72 * PC1 + 1.17 * PC2 \qquad (2)$$

In general, the model is rather accurate, with root-mean-squared error values (RMSE) of 3.8, 2.9, 2.7 and 2.0 µg kg^{-1} for A, Bh/Bs, C and E horizons, respectively. The values of the standardized coefficients of the model reflect the influence of each PC in the modeled Hg. In this way, PC4 is by far the most influencing variable with a standardized coefficient of 0.707, followed by PC1 and PC2 with respective standardized coefficients of 0.339 and 0.230.

The influence of each factor extracted by the PCA (wPC) in the Hg content for each soil is shown in Fig. 4. The component that contributed the most to the Hg concentrations found in the A horizons was PC4, which is related to soil organic matter variables (organic C, N and C$_p$).

Consistently, the highest weights of PC4 were obtained for the A horizons of the soils depicting the pattern I for Hg$_T$ distribution (P.1, P.2, P.3, P.20 and P.21) which, at the same time, show the largest organic C contents (see Table S1). This result agrees with the prevalence of an atmospheric Hg source and the Hg sorption ability of the reduced S groups of the soil organic matter (Khwaja et al., 2006; Skyllberg et al., 2006). Thus, in the soils with pattern I, the biogeochemical processes involving soil organic matter dynamics (Grigal, 2003; Hissler and Probst, 2006) that lead to the Hg$_T$ accumulation in the A horizons prevail upon Hg redistribution due to podzolization. On the contrary, the slight negative values of wPC1 in the A horizons would support the role of Al-organic matter associations in Hg transport to illuvial horizons as aforementioned and coinciding with previous studies (Schlütter, 1996, 1997; Biester et al., 2002; Dreher and Follmer, 2004; Nave et al., 2019; Gómez-Armesto et al., 2020b, 2021).

Most of the E horizons of the studied soils showed negative wPCs because of the absence of soil compounds able to retain the potentially mobilized Hg from the above A horizons due to podzolization. Previous studies about Hg in Podzols close to the study area (NW of the Iberian Peninsula) already pointed out similar reasons to explain the systematic low values of Hg$_T$ found in the E horizons (Gómez-Armesto et al., 2020b, 2021). Besides, the high Al$_p$/C$_p$ atomic ratio of the E horizons would favor the direct migration of Hg towards the illuvial layers.

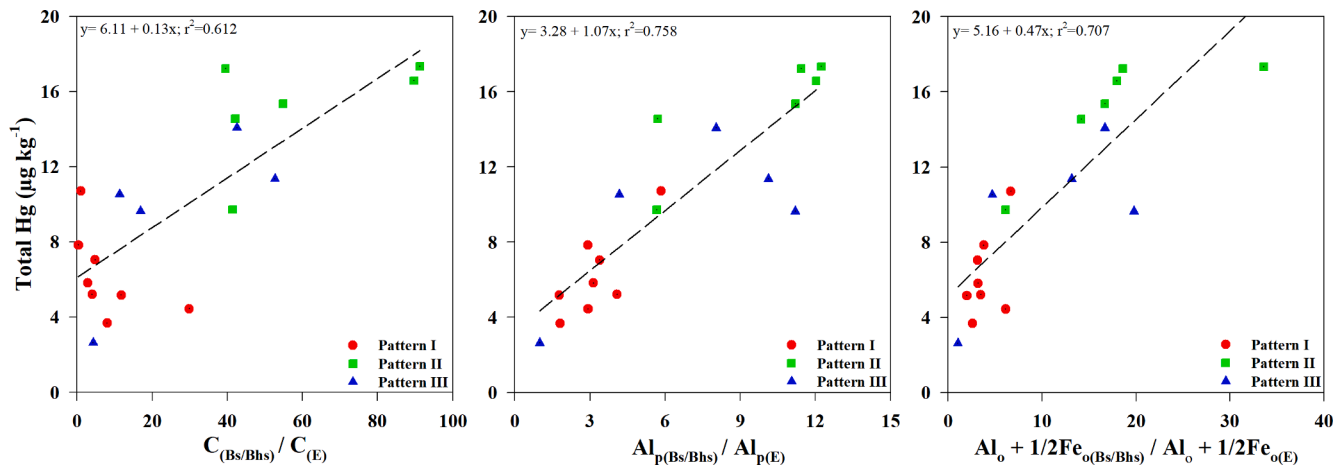The PCA showed different weights of the PCs in the prediction of the

Fig. 5. Relationships between total Hg in illuvial horizons (Bs, Bhs) and the ratios of organic C, organically-bound Al (Al_p) and non-crystalline Al plus Fe compounds ($Al_o + \frac{1}{2} Fe_o$) between illuvial (subscripts Bs, Bhs) and eluvial (subscript E) horizons depending on the type of the vertical pattern of the Hg_T distribution.

Hg content in the illuvial horizons (Fig. 4). The illuvial horizons of the soils showing pattern I did not show soil compounds influencing positively the Hg prediction, mostly soil P.1 and P.3. On the contrary, there was a noticeable contribution of wPC1 (Al compounds) and wPC4 (soil organic matter) to Hg_T prediction in soils of pattern II, while the influence of the Fe compounds (wPC2) predominated in the illuvial horizons of the soil P.26 (pattern III; Fig. 4). This distinctive behavior of the wPCs to predict Hg_T in illuvial horizons of soils with different vertical patterns seems to be closely related to the occurrence of organic matter and Al and Fe compounds, coinciding with that previously discussed for Hg immobilization in the illuvial horizons. Thus, in the illuvial horizons of soils P.1 and P.3, organic C and Al and Fe compounds (mainly as metal–organic matter associations) are almost absent (Table S1). On the other hand, illuvial horizons of the soils P.6, P.8 and P.10 are those with the highest levels of organic C and total Al-organic matter associations (estimated as Al_p) of all the studied soils (Table S1). Similarly, the Bhs horizon of the soil P.26 is remarkably high in secondary Fe compounds compared to the rest of the analyzed soils. Thus, the results of the wPCs of the illuvial horizons strengthen the participation of organic C and metal–organic matter associations in the immobilization of Hg accordingly to previous studies in Podzols (Roulet et al., 1998; Gabriel and Williamson, 2004; Richardson et al., 2013; Nave et al., 2019; Gómez-Armesto et al., 2020b, 2021).

In general, the C horizons showed negative values of the wPCs consistently with their low Hg content. However, some samples displayed positive values for wPC2 and wPC1 (Fig. 4). The positive values of wPC2, related to secondary Fe compounds, were found in the C horizon of the soil P.26 which was that with the highest Hg_T and free Fe pool (Fe_d, Table S1) among all C-horizon samples. This fact suggests that lithogenic sources could be contributing to Hg contents in the deepest soil layer of the soil P.26 to a similar extent that atmospheric deposition and podzolization did in the A and Bh/Bhs/Bh horizons, respectively. As a consequence, the vertical Hg_T distribution of pattern III was found to be uniform. Positive values of the wPC1 occurring in the C horizons of the soils with the pattern II (P.6, P.8 and P.10), suggest that secondary Al compounds can be also involved in Hg retention in these C horizons. Recently, Gómez-Armesto et al. (2020b) pointed out that secondary crystalline Al compounds (as part of the total free Al pool, Al_n) could be participating in the Hg immobilization in C horizons of Podzols, whereas the interactions between these Al compounds and Hg forming hydroxyl species were evidenced in different types of soil including Podzols (Schlütter, 1997; Guédron et al., 2009).

From the interpretations of wPCs in the E, Bh, Bhs, Bs and C horizons, the peaks of Hg in the illuvial horizons could be the result of the intense podzolization that would mobilize Hg downwards at a greater rate than

its deposition velocity in the A horizons, resulting in the defined pattern II. Contrarily, in soils with pattern III, none of the mechanisms (atmospheric deposition or podzolization) overcame each other and a more homogeneous distribution of Hg_T in the profile is observed.

From the above discussion, we consider that the different vertical Hg patterns observed among the soils from Leiria National Forest could be justified by differences in the intensity of the podzolization. The intensity of podsolization has been assessed following soil morphological features such as changes in the color parameters of Podzol horizons as for the POD Index (Schaetzl and Mokma, 1988). In other cases, the podzolization intensity is estimated as the time necessary to meet some chemical criteria to form a spodic horizon using soils of different ages, i. e. a chronosequence (Barret and Schaetzl, 1992; Mokma et al., 2004; Sauer et al., 2008: Cornelis et al., 2014). Simple chemical parameters, as the difference in Al contents between A and C horizons, is the basis of the podzolization index (Duchaufour and Souchier, 1978), whereas the amount of secondary non-crystalline Al and Fe compounds ($Al_o + \frac{1}{2} Fe_o$) is still considered criteria for spodic horizons (IUSS Working Group WRB, 2014). As the most determinant morphological and chemical changes in Podzols occur between the E and the illuvial horizons, we calculate the ratios of organic C, organically complexed Al (Al_p) and $Al_o + \frac{1}{2} Fe_o$ between both horizons as a potential approach of the podzolization degree of the studied soils. Once the aforementioned ratios were regressed against total Hg in the illuvial horizons (Fig. 5), as more organic C, Al-organic matter associations (Al_p) and secondary non-crystalline Al and Fe compounds are accumulated in the illuvial horizons compared to the E layers, greater is the amount of Hg_T accumulated in the Bs and Bhs horizons. It has been shown that an increase in organic C and secondary Al and Fe compounds (Al_p, Fe_o, Al_o, $Al_o + \frac{1}{2} Fe_o$) in illuvial horizons is the result of the progression of Podzol development with time (Mokma et al., 2004; Sauer et al., 2008) or a more intense podzolization (Jankowski, 2014; Schaetzl and Rothstein, 2016). Therefore, as more intense is the podzolization the greater are the Hg peaks in the illuvial horizons as was observed for soils with pattern II. Otherwise, under conditions less prone to podzolization, accumulation of Hg_T in uppermost soil layers will prevail leading to soils displaying pattern I as generally occurs in soils not affected by podzolization.

4. Conclusions

The podzolization is the main pedogenetic process that occurred in the studied soils, based on the distribution of organic matter and Al and Fe compounds. These components showed an impoverishment in the A and E horizons and a predominance of (Al, Fe)-organic matter associations in illuvial horizons. Three vertical patterns for the Hg distribution

along the soil profiles were observed. The pattern I included soils with the highest Hg concentrations in the A horizons, whereas soils with subsurface Hg peaks in the illuvial horizons conformed pattern II. Finally, soils of pattern III did not show any significant Hg peak, being the Hg concentration uniform through the soil profile. In this sense, a balance between two natural mechanisms, soil organic matter dynamics and podzolization, which have been occurring simultaneously in the soils studied, determined these patterns. In soils showing pattern II, in which Hg is mobilized downwards the soil profile together with organic matter and Al and Fe compounds, the precipitation of DOM-metal complexes is the more likely process responsible for Hg accumulation in these horizons. The retention of Hg in these horizons by clay minerals such as kaolinite can be discarded given its low content and the pH values of these horizons. On other hand, in soils of pattern III, none of the two mechanisms prevailed, being Hg homogeneously distributed in the profile.

The stepwise linear regression performed revealed the main components involved in the Hg accumulation in the soil profiles studied. Organic matter of different degree of humification was the most influencing soil variable, especially in the A horizons and to a lesser extent to the illuvial horizons. On the contrary, Al-humus complexes and secondary Fe compounds were the most influencing properties in the illuvial horizons. The low values of Hg in the eluvial horizons did not allow identifying any soil compound responsible for the Hg accumulation in them.

These results confirmed that the soil components present in Podzol and podzolic soils can retain Hg in subsurface soil layers, despite the high sand contents that would favor higher mobility of the pollutants through the soil profile. Therefore, the illuvial horizons of Podzols could accomplish the environmental function of a barrier that avoids the leaching of Hg to deeper soil layers and even to groundwater, where it could be transformed to the more toxic methylmercury.

Declaration of Competing Interest

The authors declare that they have no known competing financial interests or personal relationships that could have appeared to influence the work reported in this paper.

Appendix A. Supplementary material

Supplementary data to this article can be found online at https://doi.org/10.1016/j.catena.2021.105540.

References

Aastrup, M., Johnson, J., Bringmark, E., Bringmark, I., Iverfeldt, A., 1991. Occurence and transport of mercury within a small catchment area. Water Air Soil Pollut. 56, 155–167.

Abdi, H., Williams, L.J., 2010. Principal component analysis. Wiley Interdiscip. Rev. Comput. Stat. 2, 433–459.

Barret, L.R., Schaetzl, R.J., 1992. An examination of podsolization near Lake Michigan using chronofunctions. Can. J. Soil Sci. 72, 527–541.

Biester, H., Müller, G., Schöler, H.F., 2002. Binding and mobility of mercury in soils contaminated by emissions from chlor-alkali plants. Sci. Total Environ. 284, 191–203.

Blackwell, B.D., Driscoll, C.T., Maxwell, J.A., Holsen, T.M., 2014. Changing climate alters inputs and pathways of mercury deposition to forested ecosystems. Biogeochemistry 119, 215–228.

Bonifacio, E., Santoni, S., Celi, L., Zanini, E., 2006. Spodosol-histosol evolution in the Krkonoše National Park (CZ). Geoderma 131, 237–250.

Buurman, P., Jongmans, A.G., 2005. Podzolisation and soil organic matter dynamics. Geoderma 125, 71–83.

Coelho, M.R., Vidal-Torrado, P., Perez, X.L.O., Martins, V.M., Vázquez, F.M., 2010. Fractionation of aluminum by selective dissolution techniques of soils on the São Paulo State sandy coastal plain. Rev. Bras. Cienc. Solo 34, 1081–1092.

Cornelis, J.T., Weis, D., Lavkulich, L., Vermeire, M.-L., Delvaux, B., Barling, J., 2014. Silicon isotopes record dissolution and re-precipitation of pedogenic clay minerals in a podzolic soil chronosequence. Geoderma 235–236, 19–29.

Demers, J.D., Driscoll, C.T., Fahey, T.J., Yavitt, J.B., 2007. Mercury cycling in litter and soil in different forest types in the Adirondack region, New York. USA. Ecol. Appl. 17, 1341–1351.

Deurer, M., Duijnisveld, W.H.M., Böttcher, J., 2000. Spatial analysis of water characteristic functions in a sandy podzol under pine forest. Water Resour. Res. 36 (10), 2925–2935.

Dmytriw, W., Mucci, A., Lucotte, M., Pichet, P., 1995. The partitioning of mercury in the solid components of a forest soil and sediments from a hydroelectric reservoir, Northern Quebec (Canada). Water Air Soil Pollut. 80, 1099–1103.

Do Valle, C.M., Santana, G.P., Augusti, R., Egreja Filho, F.B., Windmöller, C.C., 2005. Speciation and quantification of mercury in Oxisol, Ultisol, and Spodosol from Amazon (Manaus, Brazil). Chemosphere 58, 779–792.

Dreher, G.B., Follmer, L.R., 2004. Mercury content of Illinois soils. Water Air Soil Pollut. 156, 299–315.

Du, B., Zhou, J., Zhou, L., Fan, X., Zhou, J., 2019. Mercury distribution in the foliage and soil profiles of a subtropical forest: Process for mercury retention in soils. J. Geochem. Explor. 205, 106337.

Duchaufour, P., Souchier, B., 1978. Roles of iron and clay in genesis of acid soils under a humid, temperate climate. Geoderma 20, 15–26.

Enrico, M., Le Roux, G., Maruszczak, N., Heimbürger, L.-E., Claustres, A., Fu, X., Sun, R., Sonke, J.E., 2016. Atmospheric Mercury Transfer to Peat Bogs Dominated by Gaseous Elemental Mercury Dry Deposition. Environ. Sci. Technol. 50 (5), 2405–2412.

Eusterhues, K., Rumpel, C., Kögel-Knabner, I., 2005. Organo-mineral associations in sandy acid forest soils: importance of specific surface area, iron oxides and micropores. Eur. J. Soil Sci. 56 (6), 753–763.

Eusterhues, K., Rumpel, C., Kögel-Knabner, I., 2007. Composition and radiocarbon age of HF-resistant soil organic matter in a Podzol and a Cambisol. Org. Geochem. 38 (8), 1356–1372.

FAO, 2006. Guidelines for Soil Description. Food and Agriculture Organisation of the United Nations, Rome, p. 109.

Ferro-Vázquez, C., Nóvoa-Muñoz, J.C., Costa-Casais, M., Klaminder, J., Martínez-Cortizas, A., 2014. Metal and organic matter immobilization in temperate podzols: A high resolution study. Geoderma 217–218, 225–234.

Ferro-Vázquez, C., Nóvoa-Muñoz, J.C., Klaminder, J., Gómez-Armesto, A., Martínez-Cortizas, A., 2020. Comparing podzolization under different bioclimatic conditions. Geoderma 377, 114581.

Ferro-Vázquez, C., Pérez-Rodríguez, M., Nóvoa-Muñoz, J.C., Klaminder, J., Bindler, R., Martínez Cortizas, A., 2017. Tracing Pb pollution penetration in temperate podzols. Land Degrad. Dev. 28, 2432–2445.

Fiorentino, J.C., Enzweiler, J., Angélica, R.S., 2011. Geochemistry of mercury along a soil profile compared to other elements and to the parental rock: Evidence of external input. Water Air Soil Pollut. 221, 63–75.

Fritsch, E., Balan, E., Do Nascimento, N.R., Allard, T., Bardy, M., Bueno, G., Derenne, S., Melfi, A.J., Calas, G., 2011. Deciphering the weathering processes using environmental mineralogy and geochemistry: Towards an integrated model of laterite and podzol genesis in the Upper Amazon Basin. C. R. Geosci. 343 (2–3), 188–198.

Gabriel, M.C., Williamson, D.G., 2004. Principal biogeochemical factors affecting the speciation and transport of mercury through the terrestrial environment. Environ. Geochem. Health 26, 421–434.

García-Rodeja, E., Nóvoa, J.C., Pontevedra, X., Martínez-Cortizas, A., Buurman, P., 2004. Aluminium fractionation of European volcanic soils by selective dissolution techniques. Catena 56, 155–183.

Gee, G.W. and Bauder, J.W., 1986. Particle-size analysis. In: Klute, A., (Ed.), Methods of soil analysis. Part 1. Physical and mineralogical methods, 2nd ed. SSSA Book Series 5; ASA and SSSA: Madison, WI, pp. 383-411.

Gerson, J.R., Driscoll, C.T., Demers, J.D., Sauer, A.K., Blackwell, B.D., Montesdeoca, M.R., Shanley, J.B., Ross, D.S., 2017. Deposition of mercury in forests across a montane elevation gradient: Elevational and seasonal patterns in methylmercury inputs and production. J. Geophys. Res. Biogeosci. 122, 1922–1939.

Gómez-Armesto, A., Bibián-Núñez, L., Campillo-Cora, C., Pontevedra-Pombal, X., Arias-Estévez, M., Nóvoa-Muñoz, J.C., 2018. Total mercury distribution among soil aggregate size fractions in a temperate forest podzol. Span. J. Soil Sci. 8, 57–73.

Gómez-Armesto, A., Martínez-Cortizas, A., Ferro-Vázquez, C., Méndez-López, M., Arias-Estévez, M., Nóvoa-Muñoz, J.C., 2020a. Modelling Hg mobility in podzols: Role of soil components and environmental implications. Environ. Pollut. 260, 114040.

Gómez-Armesto, A., Méndez-López, M., Pérez-Rodríguez, P., Fernández-Calviño, D., Arias-Estévez, M., Nóvoa-Muñoz, J.C., 2020b. Litterfall Hg deposition to an oak forest soil from southwestern Europe. J. Environ. Manage. 269, 110858.

Gómez-Armesto, A., Méndez-López, M., Pontevedra-Pombal, X., García-Rodeja, E., Moretto, A., Estévez-Arias, M., Nóvoa-Muñoz, J.C., 2020c. Mercury accumulation in soil fractions of podzols from two contrasted geographical temperate areas: southwest Europe and southernmost America. Geoderma 362, 114120.

Gómez-Armesto, A., Méndez-López, M., Pontevedra-Pombal, X., García-Rodeja, E., Alonso-Vega, F., Arias-Estévez, M., Nóvoa-Muñoz, J.C., 2021. Environ. Res. 193, 110552.

Gong, P., Wang, X.-P., Xue, Y.-G., Xu, B.-Q., Yao, T.-D., 2014. Mercury distribution in the foliage and soil profiles of the Tibetan forest: Processes and implications for regional cycling. Environ. Pollut. 188, 94–101.

Grand, S., Lavkulich, L.M., 2011. Depth Distribution and Predictors of Soil Organic Carbon in Podzols of a Forested Watershed in Southwestern Canada. Soil Sci. 176, 164–174.

Grigal, D.F., 2003. Mercury sequestration in forests and peatlands: A review. J. Environ. Qual. 32, 393–405.

Grimaldi, C., Grimaldi, M., Guédron, S., 2008. Mercury distribution in tropical soil profiles related to origin of mercury and soil processes. Sci. Total Environ. 401 (1–3), 121–129.

Gruba, P., Socha, J., Pietrzykowski, M., Pasichnyk, D., 2019. Tree species affects the concentration of total mercury (Hg) in forest soils: Evidence from a forest soil inventory in Poland. Sci. Total Environ. 647, 141–148.

Guédron, S. Amouroux D., Tessier E., Grimaldi C., Berail J., Perrot V. and Grimaldi, M., 2018. Mercury Isotopic Fractionation during Pedogenesis in a Tropical Forest Soil Catena (French Guiana): Deciphering the Impact of Historical Gold Mining. Environ. Sci. Technol., 52(20): 11573–11582.

Guédron, S., Grangeon, S., Jouravel, G., Charlet, L., Sarret, G., 2013. Atmospheric mercury incorporation in soils of an area impacted by a chlor-alkali plant (Grenoble, France): Contribution of canopy uptake. Sci. Tot. Environ. 445–446, 356–364.

Guédron, S., Grangeon, S., Lanson, B., Grimaldi, M., 2009. Mercury speciation in a tropical soil association; Consequence of gold mining on Hg distribution in French Guiana. Geoderma 153, 331–346.

Guédron, S., Grimaldi, C., Chauvel, C., Spadini, L., Grimaldi, M., 2006. Weathering versus atmospheric contributions to mercury concentrations in French Guiana soils. Appl. Geochem. 21, 2010–2022.

Hamilton, W., Turner, R., Ghosh, M., 1995. Effect of pH and iodide on the adsorption of mercury(II) on illite. Water Air Soil Pollut. 80, 483–486.

Hargrove, W.L., Thomas, G.W., 1981. Extraction of aluminium from aluminium-organic matter complexes. Soil Sci. Soc. Am. J. 45, 151–153.

Higashi, T., 1983. Characterisation of Al/Fe-humus complexes in Dystrandepts through comparison with synthetic forms. Geoderm 31, 277–288.

Hissler, C., Probst, J.-L., 2006. Impact of mercury atmospheric deposition on soils and streams in a mountainous catchment (Vosges, France) polluted by chlor-alkali industrial activity: The important trapping role of the organic matter. Sci. Total Environ. 361, 163–178.

Holmgren, G.G.S., 1967. A rapid citrate-dithionite extractable iron procedure. Soil Sci. Soc. Am. J. 31 (2), 210–211.

Horowitz, H.M., Jacob, D.J., Amos, H.M., Streets, D.G., Sunderland, E.M., 2014. Historical mercury releases from commercial products: Global environmental implications. Environ. Sci. Technol. 48, 10242–10250.

INMG., 1991. Normais Climatológicas da Região de "Ribatejo e Oeste", correspondentes a 1951-1980. In: O Clima de Portugal, Fasc. XLIX, Vol. 2-2.ª Região. Lisboa, Instituto Nacional de Meteorologia (INMG).

IUSS Working Group WRB, 2014. International soil classification system for naming soils and creating legends for soil maps. World Reference Base for Soil Resources 2014 World Soil Resources Reports N° 106. FAO, Rome. 181 p.

Jankowski, M., 2014. The evidence of lateral podzolization in sandy soils of Northern Poland. Catena 112, 139–147.

Jansen, B., Nierop, K.G.J., Verstraten, J.M., 2005. Mechanisms controlling the mobility of dissolved organic matter, aluminium and iron in podzol B horizons. Eur. J. Soil Sci. 56 (4), 537–550.

Jiskra, M., Wiederhold, J.G., Bourdon, B., Kretzschmar, R., 2012. Solution Speciation Controls Mercury Isotope Fractionation of Hg(II) Sorption to Goethite. Environ. Sci. Technol. 46 (12), 6654–6662.

Jiskra, M., Wiederhold, J.G., Skyllberg, U., Kronberg, R.-S., Hajdas, I., Kretzschmar, R., 2015. Mercury Deposition and Re-emission Pathways in Boreal Forest Soils Investigated with Hg Isotope Signatures. Environ. Sci. Technol. 49 (12), 7188–7196.

Juo, A.S.R., Kamprath, E.J., 1979. Copper chloride as an extractant for estimating the potentially reactive aluminium pool in acid soils. Soil Sci. Soc. Am. J. 43, 35–38.

Kaal, J., Costa-Casais, M., Ferro-Vázquez, C., Pontevedra-Pombal, X., Martínez-Cortizas, A., 2008. Soil Formation of "Atlantic Rankers" from NW Spain-A High Resolution Aluminium and Iron Fractionation Study. Pedosphere 18 (4), 441–453.

Kaiser, K., Zech, W., 1996. Defects in estimation of aluminum in humus complexes of podzolic soils by pyrophosphate extraction". Soil Sci. 161, 452–458.

Khwaja, A.R., Bloom, P.R., Brezonik, P.L., 2006. Binding constants of divalent mercury (Hg^{2+}) in soil humic acids and soil organic matter. Environ. Sci. Technol. 40, 844–849.

Klaminder, J., Bindler, R., Rydberg, J., Renberg, I., 2008. Is there a chronological record of atmospheric mercury and lead deposition preserved in the mor layer (O-horizon) of boreal forest soils? Geochim. Cosmochim. Acta 72, 703–712.

Krettek, A., Herrmann, L., Rennert, T., 2020. Podzolisation affects the spatial allocation and chemical composition of soil organic matter fractions. Soil Res. 58 (8), 713–725.

Krishna, M.P., Mohan, M., 2017. Litter decomposition in forest ecosystems: a review. Energ. Ecol. Environ. 2, 236–249.

Lin, C., Coleman, N.T., 1960. The measurement of exchangeable aluminum in soils and clays. Soil. Sci. Soc. Am. J. 24, 444–446.

Liu, R.X., Kuang, J., Gong, Q., Hou, X.L., 2003. Principal component regression analysis with SPSS. Comput. Methods Progr. Biomed. 71, 141–147.

Lundström, U.S., Van Breemen, N. and Bain, D. (2000). The podzolization process. A.

McGroddy, M.E., Daufresne, T., Hedin, L.O., 2004. Scaling of C:N: P stoichiometry in forests worldwide: Implications of terrestrial Redfied-type ratios. Ecology 85, 2390–2401.

McKeague, J.A., 1967. An evaluation of 0.1 M pyrophosphate and pyrophosphatedithionite in comparison with oxalate as extractants of the accumulation products in podzols and some other soils. Can. J. Soil Sci. 47, 95–99.

Mokma, D.L. and Buurman, P., 1982. Podzols and podsolization intemperate regions. International Soil Museum, Monograph 1. Wageningen, The Netherlands. 131 p.

Mokma, D.L., Yli-Halla, M., Lindqvist, K., 2004. Podzol formation in sandy soils of Finland. Geoderma 120 (3–4), 259–272.

Monteiro, F., Marques, P., Madeira, M., 2015. Are Podzols dominant in sand formations of the Portuguese Litoral? The case of the Leiria National Forest. Rev. Ciênc. Agrár. 38, 455–472.

Nave, L.E., Covarrubias Ornelas, A., Drevnick, P.E., Gallo, A., Hatten, J.A., Heckman, A., Matosziuk, L., Sanclements, M., Strahm, B.D., Veverica, T.J., Weiglein, T.L., Swanston, C.W., 2019. Carbon–mercury interactions in Spodosols assessed through density fractionation, radiocarbon analysis, and soil survey information. Soil Sci. Soc. Am. J. 83, 190–202.

Navrátil, T., Hojdová, M., Rohovec, J., Peníżek, V., Varilová, Z., 2009. Effect of fire on pools of mercury in forest soil, central Europe. Bull. Environ. Contam. Toxicol. 83, 269–274.

Navrátil, T., Shanley, J., Rohovec, J., Hojdová, M., Peníżek, V., Buchtová, J., 2014. Distribution and pools of mercury in Czech forest soils. Water Air Soil Pollut. 225, 1829.

Navrátil, T., Shanley, J.B., Rohovec, J., Oulehle, F., Šimecek, M., Houška, J., Cudlín, P., 2016. Soil mercury distribution in adjacent coniferous and deciduous stands highly impacted by acid rain in the Ore Mountains, Czech Republic. Appl. Geochem. 75, 63–75.

Neubauer, E., Schenkeveld, W.D.C., Plathe, K.L., Rentenberger, C., von der Kammer, F., Kraemer, S.M., Hofmann, T., 2013. The influence of pH on iron speciation in podzol extracts: Iron complexes with natural organic matter, and iron mineral nanoparticles. Sci. Total Environ. 461–462, 108–116.

Nierop, K.G.J., Jansen, B., Verstraten, J.M., 2002. Dissolved organic matter, aluminium and iron interactions: Precipitation induced by metal/carbon ratio, pH and competition. Sci. Total Environ. 300, 201–211.

Obrist, D., Pokharel, A.K., Moore, C., 2014. Vertical profile measurements of soil air suggest immobilization of gaseous elemental mercury in mineral soil. Environ. Sci. Technol. 48 (4), 2242–2252.

Parfjtt, R.L., Childs, C.W., 1988. Soil Chemistry and Mineralogy Estimation of Forms of Fe and Al: A Review, and Analysis of Contrasting Soils by Dissolution and Moessbauer Methods. Aust. J. Soil Res. 26, 121–144.

Peech, M., Alexander, L.T., Dean, L.A., Reed, J.F., 1947. Methods of soil analysis for soil fertility investigations vol. 757.

Peña-Rodríguez, S., Pontevedra-Pombal, X., Fernández-Calviño, D., Taboada, T., Arias-Estévez, M., Martínez-Cortizas, A., Nóvoa-Muñoz, J.C., García-Rodeja, E., 2012. Mercury content in volcanic soils across Europe and its relationship with soil properties. J. Soils Sediments 12, 542–555.

Peña-Rodríguez, S., Pontevedra-Pombal, X., Gayoso, E.G.R., Moretto, A., Mansilla, R., Cutillas-Barreiro, L., Arias-Estévez, M., Nóvoa-Muñoz, J.C., 2014. Mercury distribution in a toposequence of sub-Antarctic forest soils of Tierra del Fuego (Argentina) as consequence of the prevailing soil processes. Geoderma 232–234, 130–140.

Peretyazhko, T., Charlet, L., Grimaldi, M., 2006. Production of gaseous mercury in hydromorphic soils in the presence of ferrous iron: a laboratory study. Eur. J. Soil Sci. 57 (2), 190–199.

Poissant, L., Casimir, A., 1998. Water-air and soil-air exchange rate of total gaseous mercury measured in background sites. Atmos. Environ. 32 (5), 883–893.

Qian, J., Skyllberg, U., Frech, W., Bleam, W.F., Bloom, P.R., Petit, P.E., 2002. Bonding of methyl mercury to reduced sulfur groups in soil and stream organic matter as determined by x-ray absorption spectroscopy and binding affinity studies. Geochim. Cosmochim. Acta 66 (22), 3873–3885.

Qin, F., Ji, H., Li, Q., Guo, X., Tang, L., Feng, J., 2014. Evaluation of trace elements and identification of pollution sources in particle size fractions of soil from iron ore areas along the Chao River. J. Geochem. Explor. 138, 33–49.

Regelink, I.C., Voegelin, A., Weng, L., Koopmans, G.F., Comans, R.N.J., 2014. Characterization of Colloidal Fe from Soils Using Field-Flow Fractionation and Fe K-Edge X-ray Absorption Spectroscopy. Environ. Sci. Technol. 48 (8), 4307–4316.

Rennert, T., 2019. Wet-chemical extractions to characterize pedogenic Al and Fe species – a critical review. Soil Res. 57, 1–16.

Richardson, J.B., Aguirre, A.A., Buss, H.L., Toby O'Geen, A., Gu, X., Rempe, D.M., Richter, D.D.B., 2018. Mercury sourcing and sequestration in weathering profiles at six critical zone observatories. Global Biogeochem. Cycles 32, 1542–1555.

Richardson, J.B., Friedland, A.J., Engerbretson, T.R., Kaste, J.M., Jackson, B.P., 2013. Spatial and vertical distribution of mercury in upland forest soils across the northeastern United States. Environ. Pollut. 182, 127–134.

Rothstein, D.E., Toosi, E.R., Schaetzl, R.J., Grandy, A.S., 2018. Translocation of Carbon from Surface Organic Horizons to the Subsoil in Coarse-Textured Spodosols: Implications for Deep Soil C Dynamics. Soil Sci. Soc. Am. J. 82 (4), 969–982.

Roulet, M., Lucotte, M., 1995. Geochemistry of mercury in pristine and flooded ferralitic soils of a tropical rain forest in French Guiana. South America. Water Air Soil Pollut. 80, 1079–1088.

Roulet, M., Lucotte, M., Saint-Aubin, A., Tran, S., Rhéault, I., Farella, N., De Jesus Da Silva, E., Dezencourt, J., Sousa Passos, C.-., Santos Soares, G., Guimarães, J.-.D., Mergler, D. and Amorim, M., 1998. The geochemistry of mercury in central Amazonian soils developed on the Alter-do-Chao formation of the lower Tapajos River Valley, Para state, Brazil. Sci. Total Environ., 223:1-24.

Różański, S.Ł., Castejón, J.M.P., Fernández, G.G., 2016. Bioavailability and mobility of mercury in selected soil profiles. Environ. Earth Sci. 75, 1065.

Rutter, A.P., Schauer, J.J., Shafer, M.M., Creswell, J.E., Olson, M.R., Robinson, M., Collins, R.M., Parman, A.M., Katzman, T.L., Mallek, J.L., 2011. Dry deposition of gaseous elemental mercury to plants and soils using mercury stable isotopes in a controlled environment. Atmos. Environ. 45 (4), 848–855.

Sarkar, D., Essington, M.E., Misra, K.C., 1999. Adsorption of mercury(II) by variable charge surfaces of quartz and gibbsite. Soil Sci. Soc. Am. J. 63, 1626–1636.

Sarkar, D., Essington, M.E., Misra, K.C., 2000. Adsorption of mercury(II) by kaolinite. Soil Sci. Soc. Am. J. 64, 1698–1975.

Sauer, D., Schülli-Maurer, I., Sperstad, R., Sørensen, R., Stahr, K., 2008. Podzol development with time in sandy beach deposits in southern Norway. J. Plant Nutr. Soil Sci. 171, 483–497.

Sauer, D., Sponagel, H., Sommer, M., Giani, L., Jahn, R., Stahr, K., 2007. Podzol: Soil of the year 2007. A review on its genesis, occurrence, and functions. J. Plant Nutr. Soil Sci. 170, 581–597.

Schaetzl, R.J., Mokma, D.L., 1988. A numerical index of podzol and podzolic soil development. Phys. Geograph. 9, 232–246.

Schaetzl, R.J., Rothstein, D., 2016. Temporal variation in the strength of podzolization as indicated by lysimeter data. Geoderma 282, 26–36.

Schaetzl, R.J., Luehmann, M.D., Rothstein, D., 2015. Pulses of Podzolization: The Relative Importance of Spring Snowmelt, Summer Storms, and Fall Rains on Spodosol Development. Soil Sci. Soc. Am. J. 79 (1), 117–131.

Schlüter, K., 1996. Translocation of 203Hg labelled HgCl2 and CH3HgCl in an Iron-Humus Podzol studied by radio-analytical techniques. Z. Pflanzenern, Bodenkunde, p. 159.

Schlüter, K., 1997. Sorption of inorganic mercury and monomethyl mercury in an iron-humus podzol soil of southern Norway studied by batch experiments. Environ. Geol. 30, 266–279.

Schuster, E., 1991. The behavior of mercury in the soil with special emphasis on complexation and adsorption processes- a review of the literature. Water Air Soil Poll. 56, 667–680.

Schwesig, D., Matzner, E., 2000. Pools and fluxes of mercury and methylmercury in two forested catchments in Germany. Sci. Total Environ. 260, 213–223.

Sheehan, K., Fernandez, I., Kahl, J., Amirbahman, A., 2006. Litterfall Mercury in Two Forested Watersheds at Acadia National Park, Maine, USA. Water Air Soil Poll. 170 (1), 249–265.

Skjemstad, J.O., Fitzpatrick, R.W., Zarcinas, B.A., Thompson, C.H., 1992. Genesis of podzols on coastal dunes in southern Queensland. II*. Geochemistry and forms of elements as deduced from various soil extraction procedures. Aust. J. Soil Res. 30, 615–644.

Skyllberg, U., Bloom, P.R., Qian, J., Lin, C.-M., Bleam, W.F., 2006. Complexation of mercury(II) in soil organic matter: EXAFS evidence for linear two-coordination with reduced sulfur groups. Environ. Sci. Technol. 40, 4174–4180.

Spielvogel, S., Prietzel, J., Kögel-Knabner, I., 2008. Soil organic matter stabilization in acidic forest soils is preferential and soil type-specific. Eur. J. Soil. Sci. 59 (4), 674–692.

Tolpeshta, I.I., Sokolova, T.A., 2009. Aluminum compounds in soil solutions and their migration in podzolic soils on two-layered deposits. Soil Chem. 42, 24–35.

Valerio, M.W., McDaniel, M.W.P.A., Gessler, P.E., 2016. Distribution and properties of podzolized soils in the northern Rocky Mountains. Soil Sci. Soc. Am. J. 80 (5), 1308–1316.

Wang, X., Yuan, W., Lin, C.J., Zhang, L., Zhang, H., Feng, X., 2019. Climate and vegetation as primary drivers for global mercury storage in surface soil. Environ. Sci. Technol. 53, 10665–10675.

Waroszewski, J., Kalinski, K., Malkiewicz, M., Mazurek, R., Kozlowski, G., Kabala, C., 2013. Pleistocene-Holocene cover-beds on granite regolith as parent material for Podzols — An example from the Sudeten Mountains. Catena 104, 161–173.

Waroszewski, J., Malkiewicz, M., Mazurek, R., Labaz, B., Jezierski, P., Kabala, C., 2015. Lithological discontinuities in Podzols developed from sandstone cover beds in the Stolowe Mountains (Poland). Catena 126, 11–19.

Xin, M., Gustin, M.S., 2007. Gaseous elemental mercury exchange with low mercury containing soils: Investigation of controlling factors. Appl. Geochem. 22, 1451–1466.

Yin, R., Gu, C., Feng, X., Hurley, J.P., Krabbenhoft, D.P., Lepak, R.F., Zhu, W., Zheng, L., Hu, T., 2016. Distribution and geochemical speciation of soil mercury in Wanshan Hg mine: Effects of cultivation. Geoderma 272, 32–38.

Yu, X., Driscoll, C.T., Warby, R.A.F., Montesdeoca, M., Johnson, C.E., 2014. Soil mercury and its response to atmospheric mercury deposition across the northeastern United States. Ecol. Appl. 24, 812–822.

Yuan, G., Soma, M., Seyama, H., Theng, B.K.G., Lavkulich, L.M., Takamatsu, T., 1998. Assessing the surface composition of soil particles from some Podzolic soils by X-ray photoelectron spectroscopy. Geoderma 86 (3–4), 169–181.

Zbyszewski, G. and Torre de Assunção, C., 1965. Carta Geológica de Portugal (1:50 000). Notícia Explicativa da Folha 22-D, Marinha Grande. Serviços Geológicos de Portugal. Lisboa.

Zhou, J., Wang, Z., Zhang, X. and Gao, 2017. Mercury concentrations and pools in four adjacent coniferous and deciduous upland forests in Beijing, China. J. Geophys. Res.: Biogeosci., 122(5): 1260-1274.